

Bose-Einstein and Fermi-Dirac Interferometry in Particle Physics

GIDEON ALEXANDER

School of Physics and Astronomy
Raymond and Beverly Sackler Faculty of Exact Sciences
Tel-Aviv University, Tel-Aviv 69978, Israel

Abstract

The application of the Bose-Einstein and Fermi-Dirac interferometry to multi-hadron final states of particle reactions is reviewed. The underlying theoretical concepts of particle interferometry is presented where a special emphasis is given to the recently proposed Fermi-Dirac correlation analysis. The experimental tools used for the interferometry analyses and the interpretation of their results are discussed in some details. In particular the interpretation of the dimension r , as measured from the interferometry analysis, is investigated and compared to that measured in heavy-ion collisions. Finally the similarity between the dependence of r on the hadron mass and the interatomic separation on the atomic mass in Bose condensates is outlined.

Contents

1	Introduction	2
2	Basic concepts in particle interferometry	4
2.1	The Bose-Einstein correlation of two hadrons	4
2.2	The Kopylov-Podgoretskii parametrisation	6
2.3	Higher order Bose-Einstein correlations	7
2.4	Bose-Einstein correlation in two and three dimensions	9
3	Fermi-Dirac correlation	10
3.1	The spin-spin correlation	11
3.2	The phase space density approach	13
4	Experimental procedure and data analysis	14
4.1	Choice of the reference sample	15
4.1.1	Reference samples derived from the data	15
4.1.2	Monte Carlo generated reference samples	16
4.2	Final state interactions	18
4.2.1	The Coulomb effect	18
4.2.2	Strong final state interactions	19
5	The 1-Dimensional correlation results	19
5.1	The $\pi\pi$ Bose-Einstein correlation	19
5.2	The $K^\pm K^\pm$ and $K_S^0 K_S^0$ systems	21
5.3	Isospin invariance and generalised Bose-Einstein correlation	24
5.4	Observation of higher order Bose-Einstein correlations	25
5.5	Experimental results from Fermi-Dirac correlation analyses	26
6	The r dependence on the hadron mass	27
6.1	The $r(m)$ description in terms of the Heisenberg relations	28
6.2	QCD description of $r(m)$ via the virial theorem	29
7	Results from multi-dimensional Bose-Einstein correlation analyses	31
7.1	$r_{\mathbf{z}}(\mathbf{m}_{\mathbf{T}})$ description in terms of the Heisenberg relations	32
7.2	Application of the Bjorken-Gottfried relation to $r(m_T)$	34
7.3	$r(m)$ and the interatomic separation in Bose condensates	34
8	On the relation between r and the emitter size	37
8.1	The r dependence on the number of emitting sources	39
9	Summary and conclusions	40

1 Introduction

The two-particle *intensity* interferometry (*intensity* correlation) method has been worked out and exploited for the first time in the 1950's by Hanbury-Brown and Twiss (HBT) [1–3] to correlate intensity of electro-magnetic radiation, arriving from extraterrestrial radio-wave sources, and thus measure the angular diameter of stars and other astronomical objects. This method rests on the fact that bosons obey the Bose-Einstein statistics so that the symmetrisation of the multi-particle wave function affects the measured many-particle coincident spectra to lead to an enhancement, relative to the single particle spectra, whenever they are emitted close by in time-phase space. Thus the interest in the Bose-Einstein correlation properties was not only restricted to their fundamental quantum theoretical aspects but above all as a tool in the study of the properties and spatial extent of sources emitting radiation and particles in the fields of astronomy, and non-perturbative QCD aspects of particles and nuclei interactions.

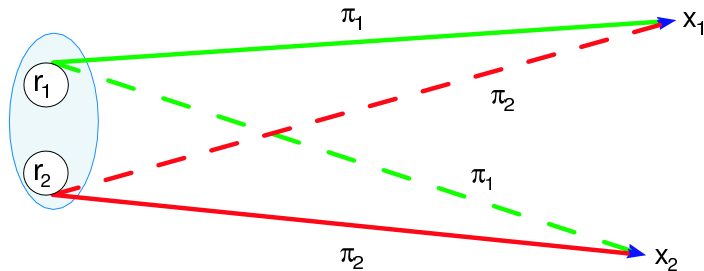


Figure 1: The two indistinguishable diagrams that describe the emission of two identical bosons, π_1 and π_2 , emerging from the two points, r_1 and r_2 , which lie within an emitter volume, and are detected at the positions x_1 and x_2 .

The difference between the *intensity* interferometry and the conventional *amplitude* interferometry can be illustrated [4,5] with the help of Fig. 1. Consider a finite source which emits two indistinguishable particles from the positions r_1 and r_2 which are later observed at positions x_1 and x_2 . In an *amplitude* interferometry the positions x_1 and x_2 could be a slit through which the emitted particles pass. The particles could then produce an interference pattern which will depend on the relative phase of the particle's amplitude as measured at x_1 and x_2 . In an *intensity* interferometry a normalised correlation function $\tilde{K}(1,2)$ of the particles **1** and **2** is formed from the average number $\langle n_{1,2} \rangle$ of counts where n_1 and n_2 are detected simultaneously at x_1 and x_2 :

$$\tilde{K}(1,2) = \frac{\langle n_{1,2} \rangle}{\langle n_1 \rangle \langle n_2 \rangle} - 1. \quad (1)$$

The correlation function is thus proportional to the intensity of the particles at x_1 and x_2 . Because of the symmetrisation of their wave function, identical particles can have a nonzero correlation function even if the particles are otherwise noninteracting.

As can be expected *intensity* interferometry is closely related to the *amplitude* interferometry which essentially measures the square of the amplitudes A_1 and A_2 falling on the detectors x_1 and x_2 :

$$|A_1 + A_2|^2 = |A_1|^2 + |A_2|^2 + (A_1^* A_2 + A_1 A_2^*),$$

where the last term is the *fringe visibility* denoted by V , which is the part of the signal which is sensitive to the separation between the emission points. Averaged over random variations its

square is given by the product of the intensities landing on the two detectors:

$$\langle V^2 \rangle = 2\langle |A_1|^2 |A_2|^2 \rangle + \langle A_1^{*2} A_2^2 \rangle + \langle A_1^2 A_2^{*2} \rangle \rightarrow 2\langle I_1 I_2 \rangle .$$

Since the last two terms of the $\langle V^2 \rangle$ expression vary rapidly and average to zero, $\langle V^2 \rangle$ is proportional to the time averaged correlation of the product of the two intensities (see e.g. Ref. [6]).

The Bose-Einstein correlation (BEC) analysis method was for the first time introduced in 1959/60 by Goldhaber, Goldhaber, Lee and Pais (GGLP) [7,8] to the hadron sector in order to study the time-space structure of identical pions produced in particle interactions. Their observation of a BEC enhancement of pion-pairs emerging from $\bar{p}p$ annihilations at small relative momenta was parametrised in terms of the finite spatial extension of the $\bar{p}p$ source and the finite localisation of the decay pions. The momentum range of the enhancement could then be related to the size of the particle source in space coordinates. Since then the boson interferometry has been used extensively in variety of particle interactions and over a wide range of energies.

In the mid 1990's the boson intensity interferometry measurement method has been extended to the spin 1/2 baryon sector utilising the Fermi-Dirac statistical properties and in particular the Pauli exclusion principle [9]. Already the results from the first attempt to study the Fermi-Dirac correlation (FDC) of the $\Lambda\Lambda$ and $\bar{\Lambda}\bar{\Lambda}$ pairs, emerging from the decay of the gauge Z^0 boson, indicated that the spatial extension of the hadron source is strongly dependent on its mass.

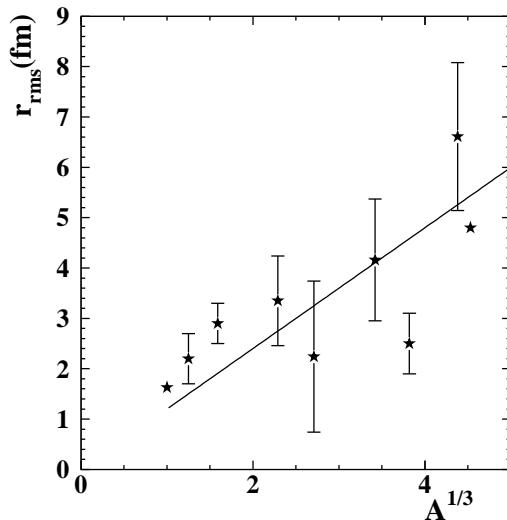


Figure 2: An early compilation of values obtained for the emitter dimension r_{rms} , extracted from interferometry analyses of identical charged pion-pairs produced in heavy ion collisions are displayed as a function of $A^{1/3}$ where A is the atomic number of the projectile. The values are taken from Ref. [10] and whenever more than one value is quoted for a given projectile nucleus, the plotted data points represent the average weighted values. The solid line represents the relation $r_{rms} = 1.2 \times A^{1/3}$ fm.

In parallel to the BEC studies of hadronic final states produced in particle reactions, extensive pion-pair correlation analyses were and are applied to heavy ion collisions in order to explore the characteristics of these rather complex reactions [6, 11, 12]. A compilation, taken

from Ref. [10], of the spatial dimension, r_{rms} , extracted from the BEC of two identical charged pions emerging from nucleus-nucleus collisions, is shown in Fig. 2 as a function of $A^{1/3}$ where A is the atomic number of the projectile nucleus. As seen in Fig. 2, r_{rms} increases more or less linearly with $A^{1/3}$. Moreover, as seen from the figure, the line $r_{rms} = 1.2 \times A^{1/3}$ fm, which corresponds to the dependence of the nucleus radius on its atomic number A , follows rather well the BEC derived spatial dimensions. This observation, as well as the results from the HBT analyses in astronomy, led to the expectation that BEC should also render information on the geometrical extension of the hadron emitter source in particle collisions.

The main purpose of the present report is to cover the field of BEC analyses applied to hadrons produced in particle collisions and only refer to heavy ion reactions whenever a comparison between the two classes of reactions is of a particular interest. A special emphasis is given to recent developments in the particle interferometry such as the inclusion of identical fermion correlations and the new results concerning the spatial dimension dependence on the hadron mass. Furthermore, the report is aimed mainly to cover the experimental aspects of the BEC and FDC interferometry and their direct physics implication and achievements while trying to restrict the theoretical discussions to essentials so as not to overburden the non-expert reader.

The organisation of this report is as follows. The basic concepts of bosons and fermions interferometry are discussed in sections 2 and 3. In section 4 details concerning the experimental aspects of the correlation measurements are described. Results obtained from the 1-dimensional correlation analyses are summarised in section 5. The observation that the spatial dimension deduced from the correlation measurements depends on the hadron mass is evaluated in section 6 and conceivable grounds for this behaviour are discussed. Results obtained from the multi-dimensional correlation analyses are dealt with in section 7 and a relation between interatomic separation in Bose condensates and the spatial dimension of hadrons emerging in high energy reaction is illustrated. In section 8 the question concerning the interpretation of the BEC and FDC deduced geometrical dimension is discussed. Finally a summary is presented in section 9.

2 Basic concepts in particle interferometry

2.1 The Bose-Einstein correlation of two hadrons

In deriving the main expressions used for the boson interferometry we follow closely Ref. [13]. As it is well known in quantum mechanics the interchange of two out of N indistinguishable bosons does not change the wave function describing this multi-boson state. This feature of the Bose-Einstein statistics means that the state Ψ has the property that

$$\Psi(1, 2, \dots, N) = \Psi(2, 1, \dots, N) ,$$

which leads to an interference term in $|\Psi|^2$ that enhances near in time-phase space the production of indistinguishable bosons. Let us first consider a source of discrete emission points, ρ_i , each characterised by a probability amplitude $F_i(\mathbf{r})$ in the 3-vector \mathbf{r}_i phase space

$$F_i(\mathbf{r}) = \rho_i \delta^3(\mathbf{r} - \mathbf{r}_i) .$$

Next we introduce the central assumption pertaining to the BEC effect namely, the *chaotic* or the total *incoherence* limit, which corresponds to the situation where the phases of the production amplitudes wildly fluctuate in every point of space. In this limit all the phases can be set to zero. If $\psi_{\mathbf{k}}(\mathbf{r})$ is the wave function of the emitted particle, then the total probability $P(\mathbf{k})$ to observe the emission of one particle with a 3-momentum vector \mathbf{k} is given by summing up the contributions from all the i points, that is

$$P(\mathbf{k}) = \sum_i |\rho_i \psi(\mathbf{r}_i)|^2 .$$

For simplicity we will further use plane wave functions $\psi_{\mathbf{k}} \propto e^{i(\mathbf{k}\mathbf{r}+\phi)}$ where in the incoherent case we can set $\phi = 0$. Next we replace the sum by an integral so that

$$P(\mathbf{k}) = \int |\rho(\mathbf{r})|^2 d^3r . \quad (2)$$

The probability to observe two particles with momenta \mathbf{k}_1 and \mathbf{k}_2 is

$$P(\mathbf{k}_1, \mathbf{k}_2) = \int |\psi_{1,2}|^2 |\rho(\mathbf{r}_1)|^2 |\rho(\mathbf{r}_2)|^2 d^3r_1 d^3r_2 , \quad (3)$$

where $\psi_{1,2} = \psi_{1,2}(\mathbf{k}_1, \mathbf{k}_2, \mathbf{r}_1, \mathbf{r}_2)$ is the two-particle wave function.

Taking incoherent plane waves, then for two identical bosons the symmetrised $\psi_{1,2}$ is of the form

$$\psi_{1,2}^s = \frac{1}{\sqrt{2}} \left[e^{i(\mathbf{k}_1\mathbf{r}_1 + \mathbf{k}_2\mathbf{r}_2)} + e^{i(\mathbf{k}_1\mathbf{r}_2 + \mathbf{k}_2\mathbf{r}_1)} \right] \quad (4)$$

so that

$$|\psi_{1,2}^s|^2 = 1 + \cos[(\mathbf{k}_1 - \mathbf{k}_2)(\mathbf{r}_1 - \mathbf{r}_2)] = 1 + \cos[\Delta\mathbf{k}(\mathbf{r}_1 - \mathbf{r}_2)] . \quad (5)$$

Using Eqs. (2), (3) and (5) one can define a second order correlation function

$$C_2(\mathbf{k}_1, \mathbf{k}_2) \equiv \frac{P(\mathbf{k}_1, \mathbf{k}_2)}{P(\mathbf{k}_1)P(\mathbf{k}_2)} = 1 + \frac{\int \cos[\Delta\mathbf{k}(\mathbf{r}_1 - \mathbf{r}_2)] |\rho(\mathbf{r}_1)|^2 |\rho(\mathbf{r}_2)|^2 d^3r_1 d^3r_2}{P(\mathbf{k}_1)P(\mathbf{k}_2)} , \quad (6)$$

where $\Delta\mathbf{k} = \mathbf{k}_1 - \mathbf{k}_2$. Assuming that the emitter extension $\rho(\mathbf{r})$ is localised in space and time then it follows that when $\Delta\mathbf{k} = 0$ the last term of Eq. (6) can vary between the values 0 to 1. From Eq. (6) one obtains after integration (Fourier transformation)

$$C_2(\Delta\mathbf{k}) = 1 + |\rho(\Delta\mathbf{k})|^2 .$$

In many of the two-boson one dimensional BEC analyses one uses the Lorentz invariant parameter Q , defined as $Q^2 = Q_2^2 = -(q_1 - q_2)^2 \equiv M_2^2 - 4\mu^2$. Here q_1, q_2 and M_2^2 are respectively the 4-momentum vectors and the invariant mass squared of the two identical bosons of mass μ .

Thus one obtains

$$C_2(Q) = 1 + |\rho(Q)|^2 . \quad (7)$$

Assuming further that the source is described by a spherical symmetric Gaussian density distribution of emitting centres

$$\rho(r) = \rho(0) e^{-\frac{r^2}{2r_0^2}} ,$$

then the Bose-Einstein correlation function assumes the form

$$C_2(\Delta\mathbf{k}) = 1 + e^{-r_0^2 \Delta\mathbf{k}^2} .$$

In terms of the variable Q and the dimension r_G , introduced by Goldhaber et al. [7, 8], the correlation function in the completely chaotic limit is equal to

$$C_2(Q) = 1 + e^{-r_G^2 Q^2}. \quad (8)$$

In the completely coherent case it can be shown [14] that $C_2(Q) = 1$. In order to accommodate those cases where the source is not completely chaotic one introduces a chaoticity parameter λ_2 which can vary between the value 0, corresponding to a complete coherent case, to the value 1 at the total chaotic limit. Thus Eq. (8) is transformed to the GGLP form

$$C_2(Q) = N(1 + \lambda_2 e^{-r_G^2 Q^2}), \quad (9)$$

where N is added as a normalisation factor. Since the strength of the BEC effect depends also on the experimental data quality, like the purity of the identical boson sample, λ_2 is often also referred to as the BEC strength parameter. In the following, unless otherwise stated, we will denote by r the dimension values obtained from BEC analyses which used the GGLP parametrisation, that is $r \equiv r_G$. Two examples of a typical behaviour of the correlation function $C_2(Q)$ of identical charged pion-pairs are shown in Fig. 3. The first are the results of OPAL [15] where the pion-pairs were taken from the hadronic Z^0 decays and the second reported by the ZEUS collaboration [16] in their study of the deep inelastic ep scattering produced at the HERA collider.

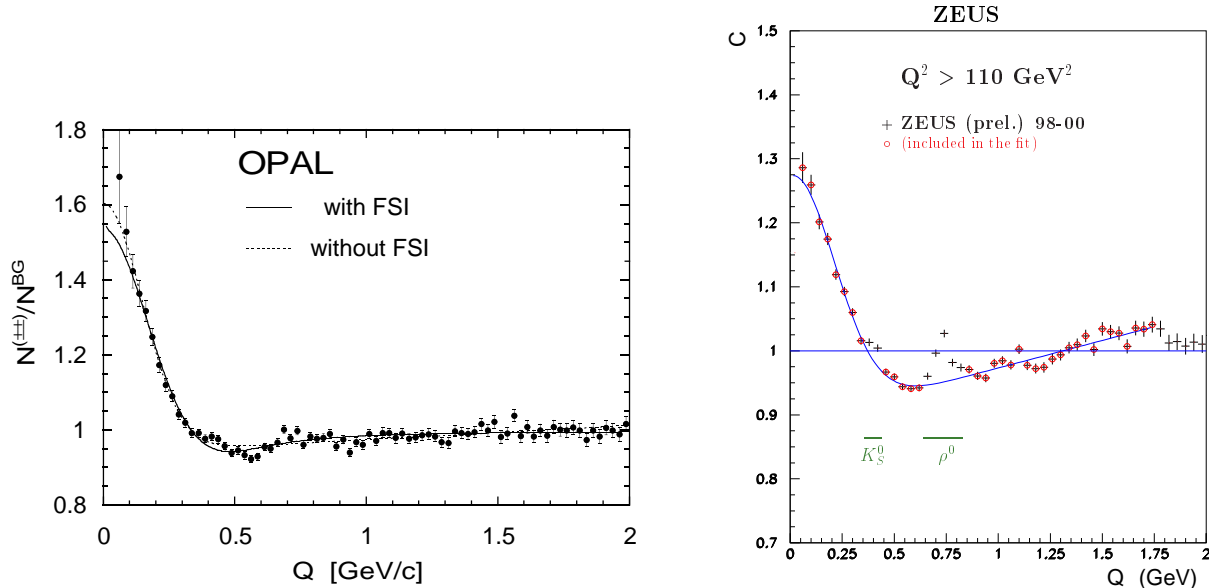


Figure 3: The $\pi^\pm\pi^\pm$ BEC as a function of Q . Left: OPAL results [15] obtained in the hadronic Z^0 decays. The solid and dashed lines represent the fit results of Ref. [17] respectively with and without the inclusion of final state interactions (see Sec. 4.2). Right: ZEUS results obtained in deep inelastic ep scattering with momentum transfer of $Q^2 > 110 \text{ GeV}^2$ [16]. The regions of K_S^0 and ρ^0 which were omitted from the fit of the correlation function $C_2(Q)$ are indicated.

2.2 The Kopylov-Podgoretskii parametrisation

In addition to the Goldhaber parametrisation, given by Eq. (9), another favourite parametrisation is that proposed by Kopylov and Podgoretskii (KP) [18–20] which corresponds to a

radiating sphere surface of radius r_{KP} with incoherent point-like oscillators of lifetime τ , namely

$$C(q_t, q_0) = 1 + \lambda [4J_1^2(q_t r_{KP}) / (q_t r_{KP}^2) / [1 + (q_0 \tau)^2]] , \quad (10)$$

where J_1 is the first-order Bessel function. Here q_0 is equal to $|E_1 - E_2|$ and $q_t = |\mathbf{q} \times \mathbf{k}| / |\mathbf{k}|$ where $\mathbf{k} = \mathbf{k}_1 + \mathbf{k}_2$, the sum of the two hadron momenta and $\mathbf{q} = \mathbf{k}_1 - \mathbf{k}_2$ is the difference between them. This correlation expression is not Lorentz invariant and its variables are calculated in the centre of mass system (CMS) of the final state hadrons. The correlation function $C(q_t, q_0)$ can be written in terms of the Goldhaber geometrical parameter r_G as [21]

$$C(q_t, q_0) = 1 + \lambda \exp[-r_G^2 q_t^2 - r_G^2 q_0^2 / (\gamma^2 - 1)] , \quad (11)$$

where γ is the γ -factor of the identical boson pair. From a comparison between Eqs. (11) and (9) it is clear that the parameters r_G and r_{KP} have different interpretations. At small q_t and q_0 , however, the parametrisation (10) can be approximated to be

$$C(q_t, q_0) = 1 + \lambda \exp[-(r_{KP}/2)^2 q_t^2 - (q_0 \tau)^2] . \quad (12)$$

From Eqs. (11) and (12) one finds the approximate relation $r_{KP} \simeq 2r_G$ which is verified experimentally. For example, in a study [22] of the BEC of the $\pi^\pm \pi^\pm$ system emerging from the decay of the Z^0 boson one obtained $r_G = 0.955 \pm 0.012(stat.) \pm 0.015(syst.)$ fm as compared to $r_{KP} = 1.778 \pm 0.023(stat.) \pm 0.036(syst.)$ fm.

In contrast to the rather simple and straightforward BEC analysis offered by the GGLP parametrisation, the KP method expects a correlation enhancement at low, near zero, q_0 values so that the analysis is carried out in several q_0 energy slices. In addition the KP formalism has an extra free parameter, $(q_0 \tau)^2$, which has to be determined through a fit to the data. For these reasons the KP correlation investigations require higher statistical data samples than those needed for the BEC analysis in the GGLP method.

2.3 Higher order Bose-Einstein correlations

A Bose-Einstein correlation enhancement is also expected to be present in identical boson systems of more than two particles when they emerge from the interaction within a small time-space region. In the search for these so called, *higher order* BEC enhancements, one has to differentiate between those produced from the lower BEC order(s) and those who are *genuine* correlations. The normalised over-all inclusive correlations of n identical bosons is given by [23]

$$R_n = \frac{\rho_n(p_1, p_2 \cdots p_n)}{\rho_1(p_1)\rho_1(p_2) \cdots \rho_1(p_n)} = \sigma^{n-1} \frac{d^n \sigma}{dp_1 dp_2 \cdots dp_n} \bigg/ \left(\frac{d\sigma}{dp_1} \frac{d\sigma}{dp_2} \cdots \frac{d\sigma}{dp_n} \right) , \quad (13)$$

where σ is the total boson production cross section, $\rho_1(p_i)$ and $d\sigma/dp_i$ are the single-boson density in momentum space and the inclusive cross section, respectively. Similarly $\rho_n(p_1, p_2 \cdots p_n)$ and $d^n \sigma / (dp_1 dp_2 \cdots dp_n)$ are respectively the density of the n -boson system and its inclusive cross section. The product of the independent one-particle densities $\rho_1(p_1)\rho_1(p_2) \cdots \rho_1(p_n)$ is referred to as the reference density distribution, or reference sample, to which the measured correlations are compared to. Specifically the inclusive two-boson density $\rho_2(p_1, p_2)$ can be written as:

$$\rho_2(p_1, p_2) = \rho_1(p_1)\rho_1(p_2) + K_2(p_1, p_2) , \quad (14)$$

where $\rho_1(p_1)\rho_1(p_2)$ represents the two independent boson momentum spectra and $K_2(p_1, p_2)$ describes the two-body correlations. In this simple case of two identical bosons the normalised density function R_2 , defined by Eq. (13), already measures the genuine two-body correlations which here (see Sec. 2.1) is referred to as the C_2 correlation function. Thus one has

$$C_2 \equiv R_2 = 1 + \tilde{K}_2(p_1, p_2), \quad (15)$$

where $\tilde{K}_2(p_1, p_2) = K_2(p_1, p_2)/[\rho_1(p_1)\rho_1(p_2)]$ is the normalised two-body correlation term which in the GGLP parametrisation defined in Eq. (9), is equal to $\lambda_2 \exp(-Q_2^2 r_2^2)$.

The inclusive correlation of three identical bosons, $\rho_3(p_1, p_2, p_3)$, includes the three independent boson momentum spectra, the two-particle correlation K_2 and the genuine three-particle correlation K_3 , namely:

$$\rho_3(p_1, p_2, p_3) = \rho_1(p_1)\rho_1(p_2)\rho_1(p_3) + \sum_{(3)} \rho_1(p_i)K_2(p_j, p_k) + K_3(p_1, p_2, p_3), \quad (16)$$

where the summation is taken over all the three possible permutations. The normalised inclusive three-body density, is then given by

$$R_3 = \frac{\rho_3(p_1, p_2, p_3)}{\rho_1(p_1)\rho_1(p_2)\rho_1(p_3)} = 1 + R_{1,2} + \tilde{K}_3(p_1, p_2, p_3). \quad (17)$$

Here

$$R_{1,2} = \frac{\sum_{(3)} \rho_1(p_i)K_2(p_j, p_k)}{\rho_1(p_1)\rho_1(p_2)\rho_1(p_3)} \quad \text{and} \quad \tilde{K}_3(p_1, p_2, p_3) = \frac{K_3(p_1, p_2, p_3)}{\rho_1(p_1)\rho_1(p_2)\rho_1(p_3)}$$

represent the mixed three-boson system in which only two of them are correlated and the three-boson correlation. In analogy to C_2 , one defines a correlation function C_3 which measures the genuine three-boson correlation, by subtracting from R_3 the term which contains the two-boson correlation contribution. Thus

$$C_3 \equiv R_3 - R_{1,2} = 1 + \tilde{K}_3(p_1, p_2, p_3), \quad (18)$$

which depends only on the genuine three-boson correlation. For the study of the three-boson correlation one often uses the variable Q_3 which, analogous to the variable Q_2^2 , is defined as

$$Q_3^2 = \sum_{(3)} q_{i,j}^2 = M_3^2 - 9\mu^2,$$

where the summation is taken over all the three different i, j boson-pairs. Here M_3^2 is the invariant mass squared of the three-boson system and μ is the mass of the single boson. From the definition of this three-boson variable it is clear that as Q_3 approaches zero so do all the three related $q_{i,j}$ values which eventually reach the region where the two-boson BEC enhancements are observed. It has been shown [24] that the genuine three-pion correlation function $C_3(Q_3)$ can be parametrised by the expression

$$C_3(Q_3) = 1 + 2\lambda_3 e^{-Q_3^2 r_3^2}, \quad (19)$$

where λ_3 is the chaoticity parameter which may assume a value between zero and one.

The method outlined here for the extraction of the three-boson BEC enhancement can in principle be extended to higher orders, however it becomes too cumbersome to be of a practical use and on top of it, it requires very high statistics data. For these reasons two other approaches have been advocated and utilised experimentally. In the first, one measures experimentally the over-all correlation, as defined by R_n in Eq. (13), and then with the help of various models one tries to extract the higher order genuine BEC parameters r_n and λ_n . Such an approach is adopted for example in references [25,26]. In the second approach one analyses the data in terms of correlation functions [27,28] known as factorial cumulant moments or, in their integrated form are referred to as the semi-invariant cumulants of Thiele which constitutes an important element in proving the central limit theorem in statistics (see e.g. [29]). Having n particles in a given domain then the corresponding factorial cumulant moments will be different from zero only if a genuine n -particle correlation exists. The shortcoming of the cumulant approach is however the fact that its results for a given higher order ($n \geq 3$) pertain to the overall genuine correlation present in the data so that the partial contribution of the genuine BEC, parametrised by r_n and λ_n is not transparent.

2.4 Bose-Einstein correlation in two and three dimensions

In the GGLP interferometry analysis the emitter shape is considered to be of a spherical shape with a Gaussian density distribution. A method to explore the possibility that the time-space extent of the particle emission region deviates from a sphere, and in fact is characterised by more than one dimension, has been recently proposed [11,30,31]. To this end the BEC analysis is carried out in the Longitudinal Centre-of-Mass System (LCMS) shown schematically in Fig. 4. This coordinate system is defined for each pair of identical bosons as the system in which

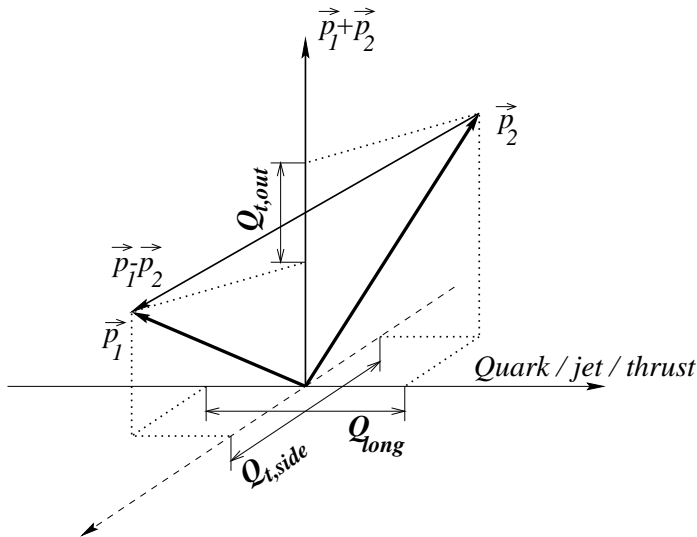


Figure 4: The Longitudinal Centre-of-Mass-System coordinates (taken from Ref. [32]).

the sum of the boson-pair 3-momenta $\mathbf{p}_1 + \mathbf{p}_2$, referred to as the *out* - axis, is perpendicular to the *thrust* (or *jet*) direction of the multi-hadron event defined as the z - axis (\equiv *long* - axis). The momentum difference of the pion-pair \mathbf{Q} is then resolved into the longitudinal direction $Q_z \equiv Q_{\parallel}$ parallel to the thrust axis, to the Q_{out} - axis which is collinear with the pair momenta sum and the third axis, Q_{side} which is perpendicular to both Q_z and Q_{out} . In this system the projections of the total momentum of the particle-pair onto the longitudinal and side directions

are equal to zero. The total Q^2 value is given by

$$Q^2 = Q_z^2 + Q_{side}^2 + Q_{out}^2(1 - \beta^2), \quad \text{where} \quad \beta = \frac{p_{1,out} + p_{2,out}}{E_1 + E_2}. \quad (20)$$

Here the indices 1 and 2 refer to the first and second boson. Since $p_{1,z} = -p_{2,z}$ one has

$$Q_z = Q_{\parallel} = p_{1,z} - p_{2,z} = 2p_{1,z} = 2p_z.$$

The difference in the emission time of the pions, which couples to the energy difference between them, appears only in the Q_{out} direction. The 3-dimension correlation function is given by

$$C_2(Q_z, Q_{side}, Q_{out}) = 1 + \lambda_2 e^{-(r_z^2 Q_z^2 + r_{side}^2 Q_{side}^2 + r_{out}^2 Q_{out}^2)}. \quad (21)$$

In many cases due to lack of sufficient statistics, one wishes to reduce the number of parameters to be fitted in the correlation function by defining the transverse component r_T in the LCMS to be $r_T^2 = r_{side}^2 + r_{out}^2$ corresponding to

$$Q_T^2 = Q_{out}^2 + Q_{side}^2.$$

Thus the correlation function, which is fitted to the data, is of the form

$$C_2(Q_z, Q_T) = 1 + \lambda_2 e^{-(r_z^2 Q_z^2 + r_T^2 Q_T^2)}, \quad (22)$$

where r_z , estimated from Eq. (22) as Q_z approaches zero, is the longitudinal geometrical radius and r_T is composed of the transverse radius and the emission time difference. The experimental findings in heavy ion collisions [33, 34], in hadron-hadron reactions [35, 36] and e^+e^- annihilations [37–39], verify the theoretical expectations of the Lund string model [40, 41] that the ratio r_T/r_z is significantly smaller than one (see Sec. 4.1.2).

The assignment of a well defined physical direction in the LCMS, such as thrust axis, allows to study in the framework of the BEC analysis an additional meaningful variable namely, the average transverse mass m_T of the two identical hadrons. This transverse mass is defined as

$$m_T = \frac{1}{2} [m_{1,T} + m_{2,T}] = \frac{1}{2} [\sqrt{m_1^2 + p_{1,T}^2} + \sqrt{m_2^2 + p_{2,T}^2}], \quad (23)$$

where the indices 1 and 2 refer to the first and second hadron.

3 Fermi-Dirac correlation

The application of two-boson correlation to the estimation of an r dimension has recently been extended to identical pairs of fermions (baryons) [9]. This extension is based on the Fermi-Dirac statistics feature which prohibit the total spin to have the value $\mathbf{S} = \mathbf{S}_1 + \mathbf{S}_2 = 1$ when the two identical fermions are in an s-wave ($\ell = 0$) state. Thus in the so called Fermi-Dirac correlation (FDC) method one can, similarly to the BEC analysis, study the contributions of the $S = 0$ and $S = 1$ states to the di-fermion system as Q approaches zero where, in the absence of di-baryon resonances, only the s-wave state survives.

The estimation of r from the rate of depletion of the $S = 1$ population as $Q \rightarrow 0$ can be achieved in two ways. The first consists of a direct measurement of the relative contributions of $S = 1$ and $S = 0$ spin states to the di-baryon system as a function of Q (see next section). An alternative method consists of a measurement of the di-baryon density decrease as Q approaches zero, assuming its origin to be due to the Pauli exclusion principle. This second method is equivalent to that used in the BEC analysis of two identical bosons.

3.1 The spin-spin correlation

If $F_0(Q)$ and $F_1(Q)$ are respectively the fraction of the $S = 0$ and the $S = 1$ contributions, at a given Q value, to the di-baryon system then one can e.g. study two correlation functions, $C_{S=0}(Q)$ and $C_{S=1}(Q)$, defined by the ratios:

$$C_0(Q) = \frac{2F_0(Q)}{F_0(Q) + F_1(Q)/3} \quad \text{and} \quad C_1(Q) = \frac{2F_1(Q)/3}{F_0(Q) + F_1(Q)/3},$$

where $F_1(Q)$ is divided by 3 to offset the statistical $2S + 1$ spin factor. At high Q values, where

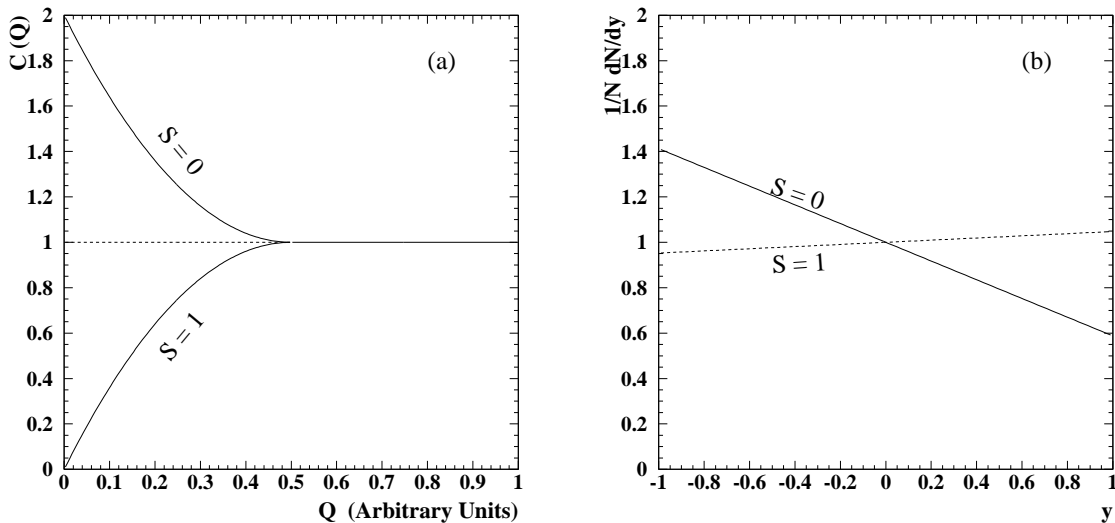


Figure 5: (a) Schematic view of the FDC functions C_0 and C_1 dependence on Q , for the $S = 0$ and $S = 1$ states, of an identical spin 1/2 two-baryon system. The dashed line represents the expectation for a baryon anti-baryon system in the absence of resonances. (b) The $(1/N)dN/dy$ behaviour of the $S = 0$ and $S = 1$ states of a two identical baryons sample.

the highest angular momentum ℓ_{max} is large, one may expect that $C_0 \cong C_1 \cong 1$ corresponding to a statistical spin mixture ensemble. On the other hand when $Q = 0$, one will observe $C_0 \approx 2$ and $C_1 \approx 0$. Thus the C_0 behaviour as a function of Q is similar to the BEC function $C_2(Q)$, of two identical mesons, which rises as the $\ell_{max} \rightarrow 0$. As for the di-baryon correlation function $C_1(Q)$ there is no parallel case in the identical charged di-boson system. One further assumes the emitter to be a sphere with a Gaussian distribution so that, analogous to the BEC parametrisation, the di-baryon correlation functions can be parametrised as [9]:

$$C_0(Q) = 1 + \lambda e^{-r^2 Q^2} \quad \text{and} \quad C_1(Q) = 1 - \lambda e^{-r^2 Q^2}.$$

Here the λ parameter, which can vary between 0 and 1, measures the strength of the effect and is mainly sensitive to the purity of the data sample. A schematic view of the dependence of C_0 and C_1 on Q is shown in Fig. 5a. The study of either C_0 or C_1 can render a value for r however, since the diminishing contribution of the $S = 1$ state is responsible for the variation of the correlation function as Q decreases, one usually analyses C_1 . Here it should be noted that unlike the BEC effect which can be extended to many-boson states, the FDC is limited to two identical fermions since already the third one is in an $\ell > 0$ state (Pauli exclusion principle).

A general method for the direct measurement of the total spin composition of any two spin 1/2 baryons system which decay weakly has been outlined in reference [9]. Here we illustrate this method (later referred as Method I) in its application to the $\Lambda\bar{\Lambda}$ and the $\Lambda\Lambda$ systems. The simplest measurable case is the one where the Λ decays into $p_1 + \pi^-$ and the other Λ , or $\bar{\Lambda}$, to $p_2 + \pi^+$ where p_i stands for the decay proton or anti-proton both of which we will further refer to as protons. Let us further denote by y the cosine of the angle (in space) between p_1 and p_2 and $\langle y \rangle$ as its average, defined in a system reached after two transformations. The first, to the CMS of the di- Λ pair and the second where each proton is transformed to the CMS of its parent Λ . To note is that at $Q = 0$ the second transformation is superfluous.

In the decay of a single Λ , the proton angular distribution with respect to the spin direction in the centre of mass, is given by [42]:

$$dw/d\cos\theta \propto 1 - \alpha_\Lambda \cos\theta, \quad (24)$$

where the parity violating parameter $\alpha_\Lambda = -\alpha_{\bar{\Lambda}}$ was measured experimentally [43] to be 0.642 ± 0.013 . Setting $x = \cos\theta$ the average $\langle x_\Lambda \rangle$ is given by:

$$\langle x_\Lambda \rangle = \frac{1}{2\pi N} \int_0^{2\pi} d\phi \int_{x_{min}}^{x_{max}} (1 - \alpha_\Lambda x) x dx \quad \text{where} \quad N = \int_{x_{min}}^{x_{max}} (1 - \alpha_\Lambda x) dx. \quad (25)$$

In particular, the average over the whole angular range from $x_{min} = -1$ to $x_{max} = +1$ yields

$$\langle x_\Lambda \rangle = -0.214 \pm 0.004 \quad \text{and} \quad \langle x_{\bar{\Lambda}} \rangle = +0.214 \pm 0.004.$$

General arguments do not allow dN/dy distribution of a two spin-1/2 hyperon system at threshold to have a y dependence higher than its first power. This means that dN/dy is of the form

$$dN/dy = A[1 + B_S y].$$

The factor B_S can then be determined independent of the total angular momentum J value at $Q = 0$ or nearby from the value of $\langle y \rangle$ using the Wigner-Eckart theorem [44,45]. Thus for the $\Lambda\Lambda$ and $\bar{\Lambda}\bar{\Lambda}$ pairs one obtains

$$B_{S=0} = -9 \langle x_\Lambda \rangle^2 = -0.4122 \quad \text{and} \quad B_{S=1} = +3 \langle x_\Lambda \rangle^2 = +0.1374.$$

As a result one then has for the $\Lambda\Lambda(\bar{\Lambda}\bar{\Lambda})$ system at, or very near, its threshold

$$dN/dy|_{S=0} \propto 1 - 0.4122y \quad \text{and} \quad dN/dy|_{S=1} \propto 1 + 0.1374y. \quad (26)$$

To note is that the $\ell = 0, S = 1$ state is forbidden by the Pauli principle. These two distinctly different distributions, are shown in Fig. 5b. In a similar way one obtains for the $\Lambda\bar{\Lambda}$ system

$$dN/dy|_{S=0} \propto 1 + 0.4122y \quad \text{and} \quad dN/dy|_{S=1} \propto 1 - 0.1374y. \quad (27)$$

Even though the Wigner-Eckart theorem is applicable to the di-baryon system at $Q = 0$, it is shown in Ref. [9] that Eqs. (26) and (27) can also be applied to at $Q > 0$ as long as the protons emerging from the Λ decays are non-relativistic. That this method can be extended even to higher Q values has been pointed out in Ref. [46]. If the parameter ϵ is defined as the fraction of the $S = 1$ contribution to the two-baryon system then it can be measured as a function of

Q by fitting the expression

$$dN/dy = (1 - \epsilon) dN/dy|_{S=0} + \epsilon dN/dy|_{S=1} , \quad (28)$$

to the data. In the case of a statistical spin mixture, ϵ is equal to 0.75 which yields a constant dN/dy distribution. This spin analysis method has the advantage that it directly measures the $S = 1$ depletion as expected from the Pauli principle. In addition it does not require any reference sample which, as is well known from the BEC analyses, is the major contributor to the systematic errors of the measurement (see Sec. 4.1). The main disadvantage of the direct spin measurement is its need for a rather large data sample. In addition, it is limited to spin 1/2 baryons which decay weakly into hadrons and thus is not applicable, for example, to pairs of protons or neutrons.

3.2 The phase space density approach

The probability to observe two particles, emitted from an interaction with 3-momenta \mathbf{k}_1 and \mathbf{k}_2 , is proportional to the square of its total wave function $\Psi_{1,2}$ which is equal to the orbital wave function $\psi_{1,2}$ times the spin part. In the case of identical spin 1/2 baryons, the function $\Psi_{1,2}$ should be anti-symmetric under the $\mathbf{1} \leftrightarrow \mathbf{2}$ exchange. Assuming plane waves and a completely incoherent emitter (i.e. the arbitrary phases can be set to zero) the symmetric and the anti-symmetric orbital wave functions are given by

$$\psi_{1,2}^s = \frac{1}{\sqrt{2}} \left[e^{i(\mathbf{k}_1 \mathbf{r}_1 + \mathbf{k}_2 \mathbf{r}_2)} + e^{i(\mathbf{k}_1 \mathbf{r}_2 + \mathbf{k}_2 \mathbf{r}_1)} \right] \quad \text{and} \quad \psi_{1,2}^a = \frac{1}{\sqrt{2}} \left[e^{i(\mathbf{k}_1 \mathbf{r}_1 + \mathbf{k}_2 \mathbf{r}_2)} - e^{i(\mathbf{k}_1 \mathbf{r}_2 + \mathbf{k}_2 \mathbf{r}_1)} \right] .$$

From these, as is shown in Sec. 2.1, one obtains for the symmetric orbital wave function, applicable to two identical hadrons

$$|\psi_{1,2}^s|^2 = 1 + \cos[(\mathbf{k}_1 - \mathbf{k}_2)(\mathbf{r}_1 - \mathbf{r}_2)] = 1 + \cos(\Delta \mathbf{k} \Delta \mathbf{r}) ,$$

whereas one obtains

$$|\psi_{1,2}^a|^2 = 1 - \cos[(\mathbf{k}_1 - \mathbf{k}_2)(\mathbf{r}_1 - \mathbf{r}_2)] = 1 - \cos(\Delta \mathbf{k} \Delta \mathbf{r}) ,$$

for the anti-symmetric orbital wave function. If we further consider a source with a spherical symmetric Gaussian density distribution [7, 8]

$$f(r) \propto e^{-r^2/(2r_0^2)} ,$$

then the rate will be

$$|\psi_{1,2}^s|^2 = 1 + e^{-r_0^2 \Delta \mathbf{k}^2} \quad \text{and} \quad |\psi_{1,2}^a|^2 = 1 - e^{-r_0^2 \Delta \mathbf{k}^2} .$$

Because of the Fermi-Dirac statistics the symmetric orbital part of the di-baryon system, $|\psi_{1,2}^s|^2$, is coupled to the anti-symmetric spin part, that is $S = 0$, whereas the anti-symmetric orbital part $|\psi_{1,2}^a|^2$ is coupled to the symmetric $S = 1$ spin part. If we further assume that at high Q values we face a statistical spin mixture ensemble, where the probability to find a di-baryon in an S state is proportional to $2S + 1$, we finally obtain for the emission rate, when properly normalised that

$$|\Psi_{1,2}|^2 = 0.25[1 + e^{-r_0^2 \Delta \mathbf{k}^2} + 3(1 - e^{-r_0^2 \Delta \mathbf{k}^2})] = 1 - 0.5e^{-r_0^2 \Delta \mathbf{k}^2} ,$$

or in its Lorentz invariant form

$$|\Psi_{1,2}(Q)|^2 = 1 - 0.5e^{-r^2Q^2} .$$

Thus one expects at $Q = 0$ a reduction in the correlation function to half of its value at the high Q region provided the following conditions are satisfied:

- At high Q values one has a statistical spin mixture ensemble;
- The di-baryon emitter is completely incoherent;
- Absence of resonance states at low Q values;
- Final states interactions can be neglected.

To accommodate in this FDC analysis method (further referred to as Method II) the cases where the emitter is not completely incoherent one introduces, as in the BEC case, a chaoticity factor λ , that can vary between 0 and +1, so that the correlation function assumes the form

$$C(Q) = N(1 - 0.5\lambda e^{-r^2Q^2}) , \tag{29}$$

where N represents a normalisation factor.

4 Experimental procedure and data analysis

Well suited reactions for a BEC analysis are those which lead to multi-hadron final states where the correlations due to resonances and conservation laws, like energy-momentum and charge balance, have minor effects. Since in these reactions the fraction of pions is the highest one, in many of the analyses one assumes that all the outgoing particles are pions and the contamination from other hadrons are accounted for by a proper correction factor and/or by an increase of the systematic error. The correlation study of kaon and proton pairs require special hadron selection criteria which tend to reduce the data statistics and introduce larger systematic errors.

In the BEC analysis the space density of the data hadron pairs dependence on Q is compared to a reference sample distribution which serves as a yardstick. The correlation function, of the form given in Eq. (9), is then fitted to the ratio of the data density distribution to that of the reference sample. To account in the GGLP parametrisation, for the so called 'long range correlations' due e.g. to energy and momentum conservation, Eq. (9) is often modified to include linear and quadratic terms in Q , namely

$$C(Q) = N(1 + \lambda e^{-r^2Q^2})(1 + \delta Q + \eta Q^2) , \tag{30}$$

where δ and η are free parameters to be determined by the fit to the data. In assessing the fitting results obtained for the r and λ parameters one has to be aware of the fact that in many cases these are not independent and a correlation between the two does exist. The weak part of the BEC analysis is undoubtedly the fact that it depends rather strongly on the chosen reference sample which thus is the main contributor to the over all systematic errors associated with the fitted parameters. The different available reference samples and the effect of the final state interactions on the BEC analysis results are discussed in some details in the following sections.

4.1 Choice of the reference sample

As mentioned above the study of the second and higher order particles' BEC enhancements requires a yardstick against which they can be detected and measured as is also evident from the $C_2(\mathbf{k}_1\mathbf{k}_2)$ definition given by Eq. (6). This yardstick is given by the so called reference sample that should be identical to the analysed data in all its aspects but free from Bose-Einstein or Fermi-Dirac statistics effects. An ideal solution to this requirement really does not exist but one has a choice of possibilities which satisfy approximately this requirement. These are divided mainly into two categories. Reference samples constructed out of the data themselves and those supplied by Monte Carlo generated samples which are subject to a full simulation of the experimental setup with its particle detection capabilities.

4.1.1 Reference samples derived from the data

The methods where the reference samples are constructed from the data themselves are often preferred as they are expected to retain many of the kinematic and dynamical data correlations such as those originating from charge, momentum and energy conservation as well as correlations arising from hadronic resonances. In the following we will briefly describe some of the data derived reference samples which, were and still are, utilised in the BEC analyses of pion-pairs.

a) In many studies of the BEC of identical charged pion-pairs ($\pi^\pm\pi^\pm$) the simplest reference sample is used. Namely, the one which is constructed out of the correlation of opposite charged pion-pairs ($\pi^\pm\pi^\mp$) present in the same data sample. This choice however has the following rather severe drawback. Whereas the $\pi^\pm\pi^\pm$ is a so called exotic system void of bosonic resonances, the origin of the $\pi^\pm\pi^\mp$ pairs may also be resonances where among them the most dominant one is the $\rho(770)$. To overcome this deficiency the expression of the correlation function, like that given by Eq. (9), is fitted to the experimental results only in the Q regions where the data is known to be free of resonances.

b) Another frequently used reference sample is the one known under the name 'mixed-event' sample. In this method one couples two identical pions each originating from a different data event. In this way one is guaranteed that no BEC effects will exist in the sample but at the price that all other kinds of correlations, like those arising from kinematic conservation laws, are also eliminated. Furthermore, as long as the data analysed is produced at low energies where the the particles emerge to a good approximation isotropically, this event mixing procedure may be satisfactory. However at higher energies where the particles emerge in hadron-jets, the mixed event technique can only be applied to two-jets events where the mixing takes place between two events with a thrust (sphericity) axes lying very nearby or alternatively after one event is rotated so that the two events axes coincide.

c) A third method in use for the generation of a reference sample, which avoids the need to rotate the event, is constructed by folding each data event along its sphericity or thrust axis so that the emerging hadrons are divided into two hemispheres. The entries to the reference sample are then all possible identical pion-pairs belonging to different hemispheres. This method, as the former one, can only be applied to two-hadron jet events.

Finally to note is that the choice of data derived reference samples for a BEC analysis

of kaon-pairs or for a FDC Method II analysis of baryon-pairs is much more restricted. For example, in the BEC analyses of $K^\pm K^\pm$ or $K_S^0 K_S^0$ pairs the data $K^\pm K^\mp$ pairs cannot be used due to the strong presence of the $\phi(1020) \rightarrow K^\pm K^\mp$ decay which lies at the very low Q range where the BEC interference is near its maximum.

4.1.2 Monte Carlo generated reference samples

Modelling of the hadron production in particle reaction plays a central role in any experimental data analysis in high energy physics. Its aim is mainly the evaluation of the various experimental deficiencies due to the imperfection of the detection system such as the geometrical acceptance, angular resolution and separation of tracks as well as the limited particle identification capabilities. In addition, the hadron production simulation serves as a yardstick against which various physics phenomena and hypotheses can be detected and measured. In this last capacity modelling of hadron production is also used extensively in the study of particle correlations.

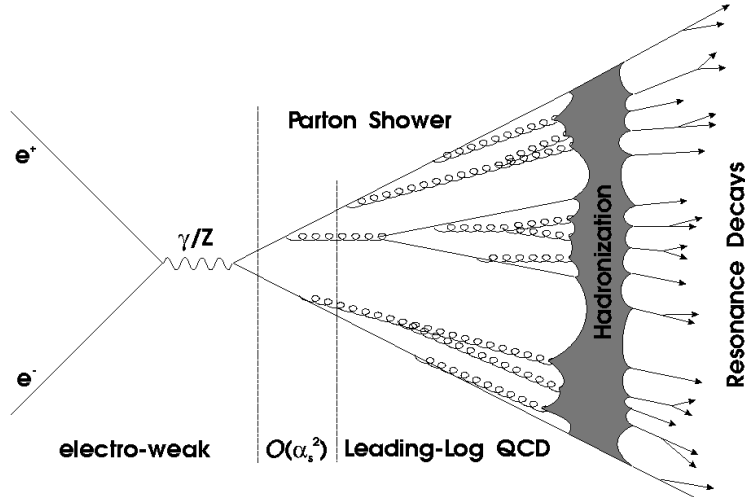


Figure 6: A schematic diagram for the production of hadrons in e^+e^- annihilation.

To illustrate the hadronisation process we show in Fig. 6 a schematic diagram for the production of hadrons in the process $e^+e^- \rightarrow Z^0/\gamma^* \rightarrow q\bar{q}$. The $q\bar{q}$, which is not directly detected, results in a relative large number of hadrons. This final step process is governed by the strong interactions and can be divided into two parts. Firstly a parton cascade develops in which the q and \bar{q} pair radiates gluons, which in turn may radiate additional gluons and split into new $q\bar{q}$ pairs. This process is followed by the hadronisation stage which emits the final observed particles. These two last stages are described in the standard model of particles and fields in terms of the Quantum Chromo Dynamics (QCD) theory where the force field between partons is the so called colour field.

At short distances and over short times the quarks and gluons can be considered as free particles where the perturbative QCD can be applied. This is not the case at the hadronisation stage where there is a need to rely on non-perturbative QCD models. One of the leading successful models, which currently is applied to many of the high energy particle reactions leading to hadronic final states, is the Lund string fragmentation model [47], shown schematically in

Fig. 7. In this Lund model the probability $|M(q\bar{q} \rightarrow h_1\dots h_n)|^2$ to emit n -hadrons is proportional e^{-bA} where A is the colour field area spanned in time-space by the primary $q\bar{q}$ pair and b is a real positive constant.

In the simplest case where the q and \bar{q} emerge in opposite directions, the colour field spanned between them is approximated by a massless relativistic string with constant energy density. These quarks oscillate back and forth and if given by collision enough energy the string will tear and a new pair of quarks will be produced. This process repeats itself until only ordinary hadrons will remain. In this model the produced hadrons are given a small transverse momentum with respect to the string axis. To note is that the production of quark pairs with $m_q > 0$ costs energy which is taken from the constant energy density string which means that they cannot be produced at the same location but will be separated by some distance proportional to their mass. The success of the Lund model stems not only from its ability to describe many of the high energy interaction features but also from the fact that it can be formulated stochastically as an iterative process and therefore is well suited for computer Monte Carlo simulation programs like the JETSET and its more recent advanced versions.

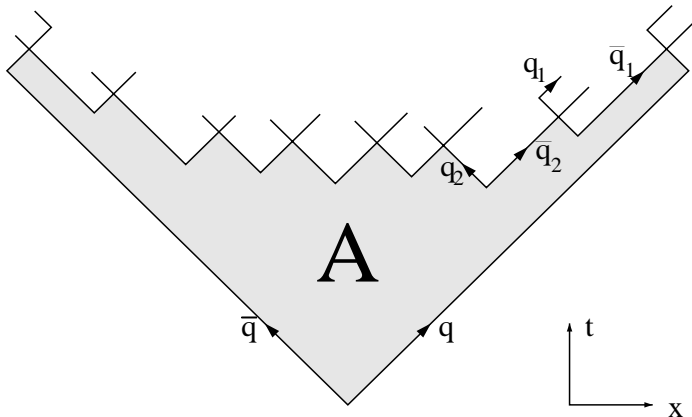


Figure 7: The hadronic decay of a Lund model string spanning the time-space area A .

Another approach to the hadronisation has been taken by the cluster model [48]. This model is based on the observation that partons generated in a branching process tend to be arranged in colour singlet clusters formed from $q\bar{q}$ pairs with limited extension in coordinate and momentum space. These clusters have masses typically of the energy scale at which the parton shower terminates. Very massive clusters decay first into lighter clusters pairs and then each cluster decays isotropically into observable hadron pairs with branching ratio determined by the density of states. This model is implemented in the HERWIG Monte Carlo program ready to be used in the experimental analyses.

At this point it is important to note that although outgoing particle tracks generated in the Monte Carlo programs do have a charge ascription their Coulomb effects are not included. In addition, all generated particles are spinless. In the Lund model derived Monte Carlo versions a facility has been added so that the Bose-Einstein statistics effects present in identical boson

system can be incorporated [49]. Another deficiency of the Monte Carlo programs is the need to adjust quite a few free parameters, like the ratio between vector and scalar resonances and their production cross sections, to the experimental findings. As a consequence, one should proceed with caution when comparing a particular effect seen in the data with the Monte Carlo program prediction. Moreover, the setting of the many free parameters may well interfere with the possibility to test the validity of the assumptions and underlying building elements of the particular hadronisation model.

4.2 Final state interactions

In the BEC and FDC analyses, final state interactions (FSI) may also play a role. There are two major FSI types. The first is the Coulomb interaction which affects the charged hadron systems and the second, the strong interaction final state which is present in both charged and neutral hadron systems. So far many of the reported BEC analyses have included the Coulomb effect whereas the strong final state interactions have in general been avoided due to their complexity and the realisation that their effect on the λ and r parameters is relatively small and can be absorbed in the overall systematic errors (see Sec. 4.2.2).

4.2.1 The Coulomb effect

In the Bose-Einstein correlation of identical charged hadrons the Coulomb repulsive force tends to reduce the enhancement signal. If $C_2^{meas}(Q)$ denotes the measured correlation of two hadrons then its relation to the true correlation $C_2(Q)$ is given by

$$C_2^{meas}(Q) = C_2(Q) \times G_2(Q) , \quad (31)$$

where $G_2(Q)$ is determined through the Gamow penetration factor [50]

$$G_2(Q) = \frac{2\pi\eta_{1,2}}{e^{2\pi\eta_{1,2}} - 1} \quad \text{where} \quad \eta_{1,2} = \epsilon_1\epsilon_2 \frac{\alpha m}{Q} . \quad (32)$$

Here ϵ_i are the charges in positron units of the hadrons, m their mass and α is the fine-structure constant. As seen from Eq. (32), the Coulomb effect increases as Q approaches zero. The measured correlation is corrected by the factor $1/G_2(Q)$ which may produce an exaggerated BEC signal [51] and therefore proper caution has to be exercised in its application. A somewhat different Coulomb correction method has been advocated in [52]. To note is that the Coulomb correction for a di-pion system is rather small (see Fig. 8) and even at $Q_2 = 0.2$ GeV does not amount to more than 2% and therefore in many reported BEC studies this correction was ignored.

The Coulomb effect on the BEC analysis of three identical charged hadrons can be expressed [54], to a good approximation, in terms of two-hadron Coulomb factors as

$$G_3(Q_3) = G_2(Q_{1,2}) \times G_2(Q_{1,3}) \times G_2(Q_{2,3}) . \quad (33)$$

Further improvements to Eq. (33) have been proposed (see e.g. Refs. [55, 56]). Unlike the di-pion case the Coulomb correction for three equally charged pions at $Q_3 = 0.25$ GeV is not negligible and, as seen in Fig. 8, amounts to about 7%.

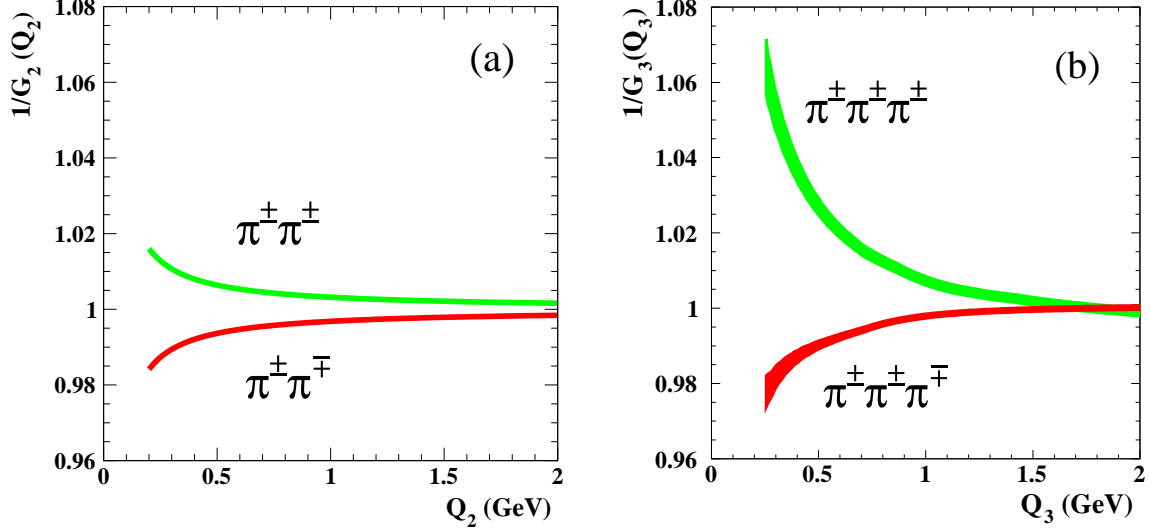


Figure 8: The Coulomb correction to the BEC correlation function [53]. (a) For two identical charged-pion systems as a function of Q_2 and (b) for the three charged pion systems as a function of Q_3 .

4.2.2 Strong final state interactions

The simultaneous effect of both the Coulomb and the strong interaction scattering of two identical charged pions on the BEC analyses have been lately worked out and reported in Ref. [17] where references to earlier studies are also included. The FSI of the strong type are limited, due to the short range of strong interaction, to the s-wave alone. For the $\pi^\pm\pi^\pm$ system the FSI dependence on Q is given by the well measured $I_{\pi\pi} = 2$ phase shift $\delta_0^{(2)}(Q)$ which can be incorporated into the BEC function.

An example for the inclusion of FSI in a BEC analysis Ref. [17] is illustrated in Fig. 3. In this figure the data points shown are the $\pi^\pm\pi^\pm$ correlation function versus Q as measured by the OPAL collaboration [15] in the hadronic Z^0 decays. The solid line represents the fit results to the BEC function including Coulomb and strong FSI whereas the dashed line is the outcome of a fit where the FSI were ignored. In a systematic study of the FSI in several BEC analyses applied to $e^+e^- \rightarrow \text{pions}$ data collected at energies on the Z^0 mass and below, it was found that in general the inclusion of the FSI tends to increase λ and decrease the r value [17].

5 The 1-Dimensional correlation results

5.1 The $\pi\pi$ Bose-Einstein correlation

The major information concerning the BEC features is coming from the $\pi^\pm\pi^\pm$ system which has been analysed in a large variety of particle reactions and over a wide range of centre of mass energies. In Table 1 results obtained from the 1-dimensional BEC analyses of two identical pions produced in e^+e^- annihilation in the energy range from 29 to 91 GeV are listed. The values for r_2 and λ_2 are divided into two groups according to the reference sample type that was used. In Method I the reference sample chosen was the data $\pi^\pm\pi^\mp$ system whereas in Method II the reference sample used was either a generated Monte Carlo sample plus a full

Table 1: The two-pion GGLP emitter dimension r_2 and the chaoticity parameter λ_2 deduced from BEC studies of e^+e^- annihilations using one or two choices for the reference sample. In Method I the reference sample was the $\pi^+\pi^-$ data sample. In Method II the reference sample used was either Monte Carlo generated events or a sample created by the event mixing technique. The given errors are the statistical and systematic errors added in quadrature. The values given are without a Coulomb correction.

$\pi^\pm\pi^\pm$ BEC		Method I		Method II	
Experiment	$\sqrt{s_{ee}}$ [GeV]	r_2 [fm]	λ_2	r_2 [fm]	λ_2
MARK II [24]	29	0.75 ± 0.05	0.28 ± 0.04	0.97 ± 0.11	0.27 ± 0.04
TPC [57]	29	–	–	0.65 ± 0.06	0.50 ± 0.04
TASSO [58]	34	0.82 ± 0.07	0.35 ± 0.03	–	–
AMY [59]	58	0.73 ± 0.21	0.47 ± 0.07	0.58 ± 0.06	0.39 ± 0.05
ALEPH [60]	91	0.82 ± 0.04	0.48 ± 0.03	0.52 ± 0.02	0.30 ± 0.01
DELPHI [61]	91	0.83 ± 0.03	0.31 ± 0.02	0.47 ± 0.03	0.24 ± 0.02
L3 [62]	91	–	–	0.46 ± 0.02	0.29 ± 0.03
OPAL [22]	91	0.96 ± 0.02	0.67 ± 0.03	0.79 ± 0.02	0.58 ± 0.01
$\pi^0\pi^0$ BEC		r_2 [fm]	λ_2	r_2 [fm]	λ_2
L3 [62, 63]	91	–	–	0.31 ± 0.10	0.16 ± 0.09
OPAL [64]	91	–	–	0.59 ± 0.11	0.55 ± 0.15

detector simulation or a sample obtained by the event mixing technique.

From the $\pi^\pm\pi^\pm$ BEC analyses results shown in Table 1 one can make the following observations. Firstly the values of r_2 are in general found to be higher in the Method I analysis than in the Method II analysis whereas the λ_2 values are roughly the same. Secondly there is no clear evidence for an r dependence on the centre of mass energy. To note is also the fact that the values of r_2 are smaller than 1 fm and their average in Method I is in the vicinity of 0.8 fm. In Method II the r values are less stable and fluctuate from experiment to experiment. It is generally believed that these fluctuations of the r values are just a reflection of the fact that different experiments used different BEC analysis procedures, namely in their data selection criteria and in their choice of the reference sample. This situation is also clearly seen in Fig. 9 where r_2 is plotted against the e^+e^- centre of mass energy, E_{cm} . In particular to note are the three r_2 values obtained in Method I for the $\pi^\pm\pi^\pm$ pairs emitted from the Z^0 gauge boson where the OPAL value differs by several standard deviations from those reported by ALEPH and DELPHI. The L3 collaboration has not given an r value in the framework of the Method I analysis. Unlike the abundant results on the $\pi^\pm\pi^\pm$ correlations the information on the BEC analyses of $\pi^0\pi^0$ pairs is very limited due to the experimental difficulties in identifying the two neutral bosons. At the same time there exists an interest in the two neutral pion system both in the framework of the string model and in the so called generalised BEC where isospin invariance is incorporated into the analysis. The two r values, obtained from the BEC analysis of the $\pi^0\pi^0$ system, present in the hadronic Z^0 decay and listed in Table 1, do not

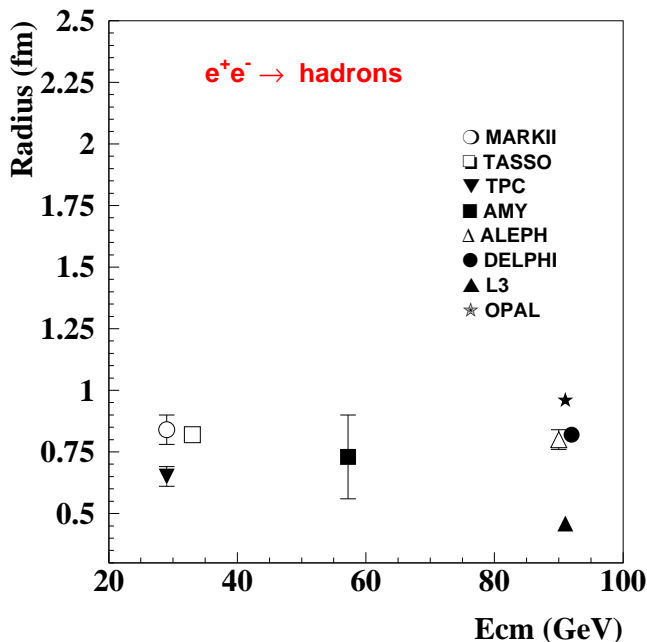


Figure 9: The emitter dimension $r_{\pi^{\pm}\pi^{\pm}}$ obtained from BEC analyses of $e^{+}e^{-}$ annihilation into hadrons versus the centre of mass energy of the $e^{+}e^{-}$ system. The values were taken from references [22, 24, 57–62] where all but TPC and L3 used a data reference sample (see also Table 1).

allow presently a meaningful comparison to the string model and isospin invariance predictions.

A compilation of $\pi^{\pm}\pi^{\pm}$ BEC parameters obtained from analyses carried out in a variety of particle reactions, other than $e^{+}e^{-}$ annihilation, is given in Table 2. Again no clear evidence can be seen for an r_2 dependence on the type of reaction and/or energy. The r values reported are, like in $e^{+}e^{-}$ annihilations, again near, or somewhat lower, than 1 fm.

The BEC of the $\pi^{\pm}\pi^{\pm}$ pairs produced in the reaction $e^{+}e^{-} \rightarrow W^{+}W^{-} \rightarrow hadrons$, where the pions are emerging from different W bosons, have been recently investigated in view of the concern that they might affect the W gauge boson mass estimation [75]. Whereas the preliminary results of DELPHI found some evidence for a BEC enhancement [76], the L3 and ALEPH collaborations have not seen any effect of this kind [77, 78].

5.2 The $K^{\pm}K^{\pm}$ and $K_S^0K_S^0$ systems

The results from BEC analyses of the $K^{\pm}K^{\pm}$ system are meager in comparison to those reported from the $\pi\pi$ BEC analyses. This is mainly due to the fact that the rate of the charged kaons is much smaller than that of the charged pions which even in the hadronic Z^0 decays amounts only to $\simeq 2.4/17$. An additional reason for the relatively poor kaon-pairs statistics stems from the need to remove from their sample contributions from protons, anti-protons and charged pions. This is achieved by applying hadron identification criteria which in most cases are effective only in a limited range of momentum. In the $e^{+}e^{-}$ annihilations on the Z^0 mass energy two $K^{\pm}K^{\pm}$ BEC analyses have been reported [79, 80]. Their extracted $r_{K^{\pm}K^{\pm}}$ values are listed in Table 4.

Table 2: A representative sample of the two-pion emitter dimension r and the chaoticity parameter λ_2 deduced from BEC studies of hadron-hadron, lepton-hadron and $\gamma\gamma$ reactions leading to multi-hadron final states. The data selection and reference samples, as well as the application of the Coulomb correction, differ from experiment to experiment. In most cases the errors given are only the statistical ones. The systematic errors are typically of the order of 10 to 20% of the measured parameter values.

$\pi^\pm\pi^\pm$ BEC analyses		Parameter	
Reaction	E_{CM} [GeV]	r_2 [fm]	λ_2
$\gamma\gamma \rightarrow h$ [24]	$< 5 >$	1.05 ± 0.08	1.20 ± 0.13
$\gamma\gamma \rightarrow 6\pi^\pm$ [65]	1.6 – 7.5	0.54 ± 0.22	0.59 ± 0.20
$\nu(\bar{\nu})N \rightarrow h$ [66]	8 – 64	0.64 ± 0.16	0.46 ± 0.16
$\mu p \rightarrow h$ [67]	23	0.65 ± 0.03	0.80 ± 0.07
$\pi^+ p \rightarrow h$ [68]	21.7	0.83 ± 0.06	0.33 ± 0.02
$pp \rightarrow h$ [69]	26	1.02 ± 0.20	0.32 ± 0.08
$pp \rightarrow h$ [70]	27.4	1.20 ± 0.03	0.44 ± 0.01
$pp \rightarrow h$ [71]	63	0.82 ± 0.05	0.40 ± 0.03
$\bar{p}p \rightarrow h$ [72]	1.88	1.04 ± 0.01	1.96 ± 0.03
$\bar{p}p \rightarrow h$ [73]	200 - 900	0.73 ± 0.03	0.25 ± 0.02
$e p \rightarrow e h$ [74]	$6 < Q_\gamma^2 < 100$ [GeV ²]	0.68 ± 0.06	0.52 ± 0.20
$e p \rightarrow e h$ [16]	$110 < Q_\gamma^2$ [GeV ²]	0.67 ± 0.04	0.43 ± 0.09

Unlike the $K^\pm K^\pm$ pairs, the origin of the $K_S^0 K_S^0$ system is not only fed from strangeness ± 2 states but also from the boson-antiboson $K^0 \bar{K}^0$ (strangeness = 0) system which in turn may be fed from the decay of resonances. Neglecting CP violation¹ we show in the following that a Bose-Einstein like threshold enhancement is nevertheless expected in the $Q(K_S^0, K_S^0)$ distribution even when its origin is the $K^0 \bar{K}^0$ system [81–84].

In general a boson-antiboson, $B\bar{B}$, pair is an eigenstate of the charge conjugation operator C . In the absence of outside constraints, one can write the probability amplitude for a given charge conjugation eigenvalue C_n as follows:

$$\frac{1}{\sqrt{2}} |B; \bar{B}\rangle_{C_n=\pm 1} = \frac{1}{2} |B(\mathbf{p}); \bar{B}(-\mathbf{p})\rangle \pm \frac{1}{2} |\bar{B}(\mathbf{p}); B(-\mathbf{p})\rangle, \quad (34)$$

where \mathbf{p} is the three momentum vector defined in the $B\bar{B}$ centre of mass system. In the $Q = 0$ limit, where the BEC effect should be maximal, \mathbf{p} is equal to zero and Eq. (34) reads

$$\frac{1}{\sqrt{2}} |B; \bar{B}\rangle_{C_n=\pm 1} = \frac{1}{2} |B(0); \bar{B}(0)\rangle \pm \frac{1}{2} |\bar{B}(0); B(0)\rangle. \quad (35)$$

This means that, at $Q = 0$, the probability amplitude for the $C_n = -1$ state (odd ℓ values) is zero whereas the $C_n = +1$ state (even ℓ values) is maximal. Here it is important to note that

¹The inclusion of CP violation effect in the following discussion is straightforward but with negligible consequences at the current experimental precision level.

these equations do hold for any spinless boson-antiboson pair such the $K^0\bar{K}^0$, the K^+K^- and the $\pi^+\pi^-$ systems. What does distinguish the $K^0\bar{K}^0$ from the other spinless boson-antiboson pairs is the simplicity by which one is able to project out the $C_n = +1$ and the $C_n = -1$ parts of the probability amplitude.

As is well known, the K^0 and the \bar{K}^0 mesons are described in terms of the two CP eigenstates, K_S^0 with $CP_n = +1$ and K_L^0 with $CP_n = -1$. From this follows that, when the $K^0\bar{K}^0$ pair is detected through their K_S^0 and K_L^0 decays, a definite eigenvalue C_n of the $K^0\bar{K}^0$ system can be selected. Thus, as Q approaches zero, an enhancement should be observed in the probability to detect $K_S^0 K_S^0$ pairs and/or $K_L^0 K_L^0$ pairs ($C_n = +1$), whereas a decrease should be seen in the probability to find $K_S^0 K_L^0$ pairs ($C_n = -1$). The BEC can thus be analysed by forming for the eigenstate $C_n = +1$ and $C_n = -1$ respectively the correlation functions:

$$C_+(Q) = \frac{2P(K_S^0 K_S^0) + 2P(K_L^0 K_L^0)}{P(K^0 \bar{K}^0)} \quad \text{and} \quad C_-(Q) = \frac{2P(K_S^0 K_L^0) + 2P(K_L^0 K_S^0)}{P(K^0 \bar{K}^0)}, \quad (36)$$

where P stands for the production rate of a given two-boson state as a function of Q .

These $C_+(Q)$ and $C_-(Q)$ dependence on Q , for $\lambda = 1$, are drawn schematically in Fig. 10. As seen, when Q approaches zero, $C(Q)$ splits into two branches. The first rises up to the value two and the other decreases to zero in such a way that their sum remains constant and equal to one at all Q values. This means, that if all the decay modes of the $K^0\bar{K}^0$ pairs are detected and used simultaneously in the same correlation analysis then, according to Eqs. (34) and (35), no BEC effect will be observed at $Q = 0$. This however should not come as a surprise if one recalls that the $K^0\bar{K}^0$ system is at the very end not composed of two identical bosons.

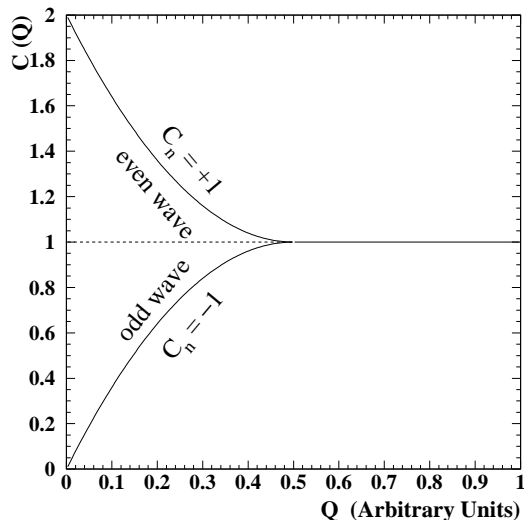


Figure 10: Schematic behaviour of the correlation functions $C(Q)$ of the $K^0 \bar{K}^0$ system given by Eq. (36). The $C_n = +1$ probability amplitude reaches the value 2 at the limit of $Q = 0$ whereas the $C_n = -1$ probability amplitude reaches the value 0. The sum of $C_n = +1$ and $C_n = -1$ remains constant down to $Q = 0$.

The interpretation of a BEC enhancement in the $K_S^0 K_S^0$ system is not straightforward as

its origin may also be the decay of the scalar $f_0(980)$ resonance. This resonance, which is mainly observed in its decay to pion-pair in the decay of the Z^0 gauge boson [85], lies within its width at the $K^0\bar{K}^0$ threshold of 995.3 MeV. Thus the low Q enhancement seen in the $K_S^0 K_S^0$ correlation at $Q \sim 0$ may be formed from the Bose-Einstein effect and/or from the $f_0(980)$ resonance decay. A possible method to disentangle the two contributions is given by isospin considerations [86] which is outlined in the following section. Values for λ and r obtained for the $K_S^0 K_S^0$ system, produced in e^+e^- annihilation on the Z^0 mass, are given in Table 4.

5.3 Isospin invariance and generalised Bose-Einstein correlation

In the sector of strong interacting hadrons where BEC and FDC analyses are performed, the isospin is a conserved quantity. In analogue to the so called generalised Pauli principle, which is the extension of that principle from two identical nucleons, the proton-proton and neutron-neutron pairs, to the proton-neutron system, one can generalise the Bose-Einstein statistics by the inclusion of the isospin invariance. This extension may relate for example, BEC results of the $\pi^\pm\pi^\pm$ pairs to those obtained for the $\pi^+\pi^0$ system. This extension was pointed out by several authors (see e.g. references [13, 87–89]) and recently was worked out in details [86] to produce concrete relations between the BEC effects of hadron systems which are connected by isospin and are proposed to be tested experimentally. So far however the concept of the generalised BEC has not been verified as it involves pion systems which include one or more neutral pions which experimentally are hard to detect and identify. However if the generalised BEC assumption is confirmed then its effect on particles correlations is not negligible. In the following we briefly discuss some aspects of the generalised BEC features and consequences.

First to note is that in many cases boson pairs, like the KK and $\pi\pi$ systems, are produced together with other hadrons, here denoted by X , from an initial state which is isoscalar to a very good approximation. These include e.g. pairs produced from an initial multi-gluon state, pairs from hadronic decays of J/ψ and Υ , or pairs produced by Z^0 decays. In some of these cases the initial state is however not pure $I=0$ but has also some contamination of an $I=1$ component which is mixed in like in those processes where the J/ψ and Υ decay to hadrons via one photon annihilation. According to the specific case methods can be applied to reduce, or even eliminate, this contamination. For example, the subsample of the $C_n = -1$ quarkonia which decays into an odd number of pions assures, due to G-parity, that the hadronic final state is in an $I=0$ state. Forming such a subsample from the hadronic Z^0 decays is not useful, but on the other hand multi-hadron final states which originate from Z^0 decays into $s\bar{s}$, $c\bar{c}$ and $b\bar{b}$ quark pairs, are in an $I=0$ state.

Several specific relations in the framework of the generalised Bose-Einstein statistics between charge and neutral K-mesons have been proposed in reference [86]. Among others, of a particular interest are those relations which have a bearing on the analysis of the enigmatic scalar $f_0(980)$ resonance, whose mass and width lie in the KK threshold region, and which has a long history regarding its nature and decay modes [43, 90–92]. For details concerning these relations the reader is advised to turn to reference [86].

Next we turn to the effect of the generalised BEC assumption on the $\pi\pi$ system. In this system there are more states and more isospin amplitudes than the two, $I=0$ and $I=1$ of the KK system. In the low Q region where only the s-wave contributes, the $\pi^+\pi^+$, $\pi^+\pi^-$ and $\pi^0\pi^0$

amplitudes depend upon only two isospin amplitudes, I=0 and I=2. Their intensities in this region satisfy a triangular inequality [86]

$$\begin{aligned}
& \sum_X \left| \sqrt{(2/3) \cdot P[i_o \rightarrow (\pi^0\pi^0)X]} - \sqrt{(1/3) \cdot P[i_o \rightarrow (\pi^+\pi^-)_e X]} \right| \leq \\
& \leq \sum_X \sqrt{P[i_o \rightarrow (\pi^\pm\pi^\pm)X]} = \sum_X \sqrt{P[i_o \rightarrow (\pi^\pm\pi^0)_e X]} \leq \\
& \leq \sum_X \left| \sqrt{(2/3) \cdot P[i_o \rightarrow (\pi^0\pi^0)X]} + \sqrt{(1/3) \cdot P[i_o \rightarrow (\pi^+\pi^-)_e X]} \right| , \tag{37}
\end{aligned}$$

where the notation $(\pi\pi)_e$ is used to indicate that only even partial waves for the $(\pi\pi)$ final state are included in the sum. Here i_o denotes an initial I=0 state and X stands for the hadrons produced in association with the two earmarked pion-pair.

In this last relation the middle line is of a particular interest as it states that at low Q values, where only the s-wave survives, the BEC enhancement in the $\pi^\pm\pi^0$ system should be equal to that present in the $\pi^\pm\pi^\pm$ pairs. Finally the BEC features of the $\pi^0\pi^0$ system should not be far from that of the $\pi^+\pi^+$ state as long as the contribution of the $\pi^\pm\pi^\mp$ to the triangle inequality relation remains small.

5.4 Observation of higher order Bose-Einstein correlations

As mentioned in Sec. 2.3, the directly measured higher order BEC are essentially limited to the case of three identical charged pions. In these analyses, the contribution from the two-hadron BEC was subtracted in each experiment with somewhat different method. The genuine $\pi^\pm\pi^\pm\pi^\pm$ BEC were also measured in the reaction $e^+e^- \rightarrow Z^0$ followed by an hadronic decay [93–95]. The experimental normalised distribution, which is marked by (a) in Fig. 11, is that found by OPAL [94] to describe the contribution to $R_3(Q_3)$, as defined in Eq. (17), from the over-all three identical charged pion BEC enhancement. In the same figure the three-pion distribution, denoted by (b), corresponds to the BEC enhancement due to the lower order BEC correlations i.e. the two-pion system. A clear evidence is seen for the genuine three-pion BEC enhancement which can be extracted by subtracting the distribution (b) from that of (a) which then allows the evaluation of r_3 .

Results for the three-boson emitter dimension are listed in Table 3 where the values of r_3 and the ratio r_3/r_2 are given. As can be seen, it does not seem to exist a significant dependence of the r_3 and r_3/r_2 values on the type and/or energy of the particles reaction.

In Ref. [24] a relation is derived between the two-pion emitter radius r_2 and the three-pion emitter radius r_3 as extracted from a fit of $R_3(Q_3)$ to the over-all (non-genuine) three-boson correlation distribution. This relation, which is based on the Fourier transform of a Gaussian shape hadron source, is given by the inequality

$$r_2/\sqrt{3} \leq r_3 \leq r_2/\sqrt{2} . \tag{38}$$

so that r_3/r_2 , lies in the range of 0.55 to 0.71. The inequality relation (38) is reduced to the equality

$$r_3 = r_2/\sqrt{2} , \tag{39}$$

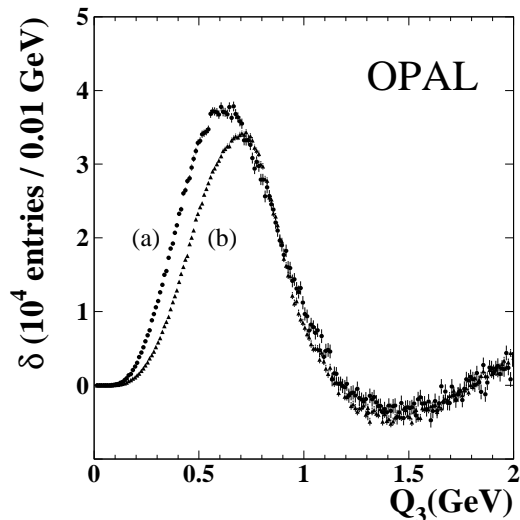


Figure 11: BEC results from an OPAL study of three identical charged pions detected in the hadronic Z^0 decays [94]. The over-all normalised BEC enhancement is described by the (a) distribution whereas distribution (b) corresponds to the three-pion BEC enhancement generated from the lower order BEC enhancement of the two-pion system.

when the emitter radius r_3 is determined from the genuine BEC distribution parametrised by $C_3(Q_3)$ so that r_3/r_2 should exactly be equal to 0.71. The experimental results, shown in Table 3, are seen to fulfil the expected relations between r_2 and r_3 and in particular the results from the genuine three-pion correlation obtained from the hadronic Z^0 decay are consistent within one to two standard deviations with the expectation of Eq. (39).

5.5 Experimental results from Fermi-Dirac correlation analyses

Until recently FDC analyses of fermion-pairs were prohibited due to the low production rate of identical di-baryons in particle reactions at low and intermediate energies. This situation changed with the commission of the LEP collider, operating on the Z^0 mass energy, where each of its four experiments have accumulated some 3 to 4 million hadronic Z^0 decays. The inclusive Z^0 decay branching ratio of ~ 0.34 Λ per event was sufficiently high to allow a FDC analysis of the Λ $\Lambda(\bar{\Lambda} \bar{\Lambda})$ and $\Lambda \bar{\Lambda}$ pairs which are free of Coulomb effects and are relatively easy identified. Results from these analyses have been reported by the OPAL [98], DELPHI [99] and ALEPH [100] collaborations using the spin-spin correlation method (see Fig. 12). The ALEPH collaboration has further repeated its analysis with Method II, i.e. with the phase space density approach and found the results of both methods to be consistent within errors (see Fig. 13). In the same figure is also shown the OPAL [101] recent $\bar{p} \bar{p}$ FDC measurement carried out in the hadronic Z^0 decays.

A summary of the measured di-baryon r values is given in Table 4 together with the average LEP1 value for the $\pi^\pm \pi^\pm$ pairs and values for the $K^\pm K^\pm$ and $K_S^0 K_S^0$ systems obtained from BEC analyses. To note is the fact, as already discussed in Sec. 5.2, that the $K_S^0 K_S^0$ pairs may also be the decay product of resonances like the $f_0(980)$, whereas the other hadron pairs listed in the Table form, so called, exotic states, that is they are in isospin 2 or strangeness ± 2

Table 3: Results for r_3 and r_3/r_2 values obtained from BEC analyses of two and three identical charged pions. Values for genuine three-pion BEC are marked by (g) otherwise they are marked by (n).

2 π and 3 π BEC analyses			Parameter	
Reaction	E_{CM} [GeV]	r_3 [fm]	r_3/r_2	
$\pi^+p, K^+p \rightarrow h$ [96]	22	0.51 ± 0.01 (g)	0.61 ± 0.12	
$pp \rightarrow h$ [97]	26	0.58 ± 0.07 (n)	0.58 ± 0.25	
$pp \rightarrow h$ [70]	27.4	0.54 ± 0.01 (n)	0.45 ± 0.07	
$pp \rightarrow h$ [71]	63	0.41 ± 0.02 (n)	0.50 ± 0.13	
$e^+e^- \rightarrow h$ [24]	3.1	0.53 ± 0.03 (n)	0.65 ± 0.17	
$e^+e^- \rightarrow \gamma\gamma$ [24]	5	0.55 ± 0.03 (n)	0.65 ± 0.20	
$e^+e^- \rightarrow h$ [24]	4–7	0.45 ± 0.04 (n)	0.63 ± 0.18	
$e^+e^- \rightarrow h$ [24]	29	0.64 ± 0.06 (n)	0.77 ± 0.25	
$e^+e^- \rightarrow h$ [58]	29–37	0.52 ± 0.07 (n)	0.59 ± 0.21	
$e^+e^- \rightarrow h$ [93]	91	0.66 ± 0.05 (g)	0.80 ± 0.16	
$e^+e^- \rightarrow h$ [94]	91	0.58 ± 0.05 (g)	0.73 ± 0.13	
$e^+e^- \rightarrow h$ [95]	91	0.65 ± 0.07 (g)	1.00 ± 0.12	

states or they belong to an identical di-baryon state. The most striking feature that emerges from the measured data listed in Table 4 is the very small r values obtained for the identical di-baryon systems which lie in the vicinity of ~ 0.15 fm, way below the values obtained for the mesons and also much smaller than the proton charge and nuclear radius [105] of $\sim 0.83 \pm 0.02$ fm. Finally the fact that the data in Table 4 utilised the same reaction at the same centre of mass energy, affords a unique opportunity to study the emitter dimension r as a function of the hadron mass. This feature is dealt with in the following sections.

6 The r dependence on the hadron mass

The r_2 dependence on the hadron mass, $r(m)$, shown in Fig. 14, exhibits a relatively strong decrease in r as the hadron mass increases, a feature which however currently rests mainly on the results obtained for the baryon-pairs. The possibility that the origin of this behaviour arises from purely kinematic considerations has been explored in Ref. [106] with the conclusion that this by itself cannot account for the rather sharp decrease of r_2 with m . Thus this r_2 dependence on the hadron mass has to be faced by all non-perturbative QCD models which attempt to describe the hadron production process. In particular $r(m)$ poses a challenge to the string approach which also constitutes a basis for the Lund model of hadronisation described in details in [47], which expects that $\partial r/\partial m > 0$ in its rudimental form. Whereas the somewhat smaller value of $r(m_K)$ as compared to that of $r(m_\pi)$, may still be acceptable, the very small r_2 values extracted from the Λ and proton pairs cannot apparently be accommodated within the Lund string approach [107].

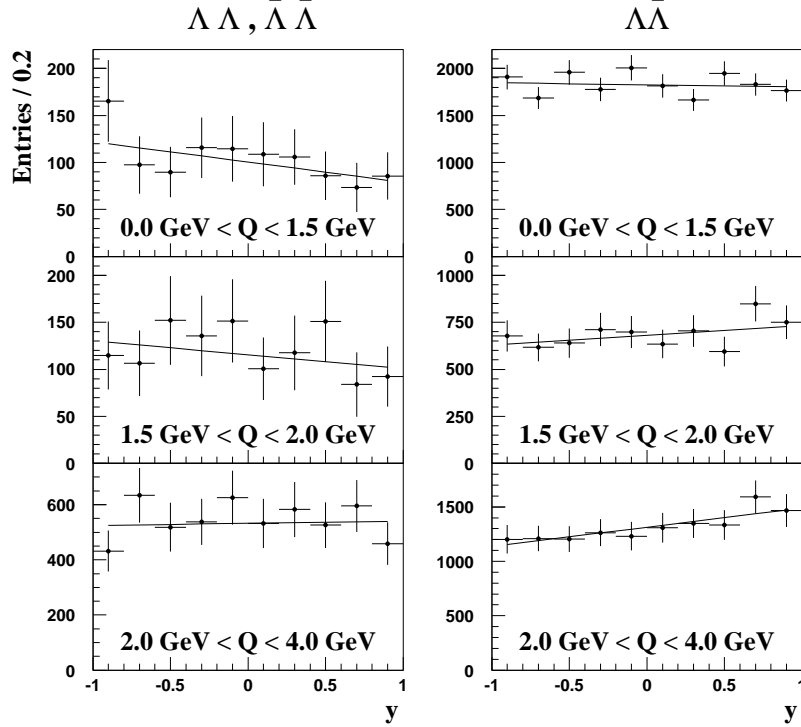


Figure 12: The ALEPH results from the spin-spin FDC analysis of the $\Lambda\Lambda$ and $\Lambda\bar{\Lambda}$ pairs observed in the hadronic Z^0 decays [100] given at several Q regions and presented in terms of dN/dy where y is the cosine angle between the two decay protons. The lines represent the best fit of Eq. (28) to the data.

6.1 The $r(m)$ description in terms of the Heisenberg relations

The maximum of the BEC and FDC effects, from which the dimension r is deduced, occurs when the Q value of the two identical hadrons of mass m approaches zero i.e., the hadrons are almost at rest in their CMS which also means that the three vector momentum difference Δp approaches zero. This motivated the attempt to link the $r(m)$ behaviour to the Heisenberg uncertainty principle [102]. From these uncertainty relations one has that

$$\Delta p \Delta r = 2 \mu v r = m v r = \hbar c , \quad (40)$$

where m and v are the hadron mass and its velocity. Here μ is the reduced mass of the di-hadron system and r is the geometrical distance between them. The momentum difference Δp is measured in GeV and $r \equiv \Delta r$ is given in Fermi units while $\hbar c = 0.197$ GeV fm. From Eq. (40) follows that

$$r = \frac{\hbar c}{m v} = \frac{\hbar c}{p} . \quad (41)$$

Simultaneously one also utilises the uncertainty relation expressed in terms of time and energy

$$\Delta E \Delta t = \frac{p^2}{m} \Delta t = \hbar , \quad (42)$$

where the ΔE is given in GeV and Δt in seconds. Thus one has

$$p^2 = \hbar m / \Delta t \quad \text{so that} \quad p = \sqrt{\hbar m / \Delta t} . \quad (43)$$

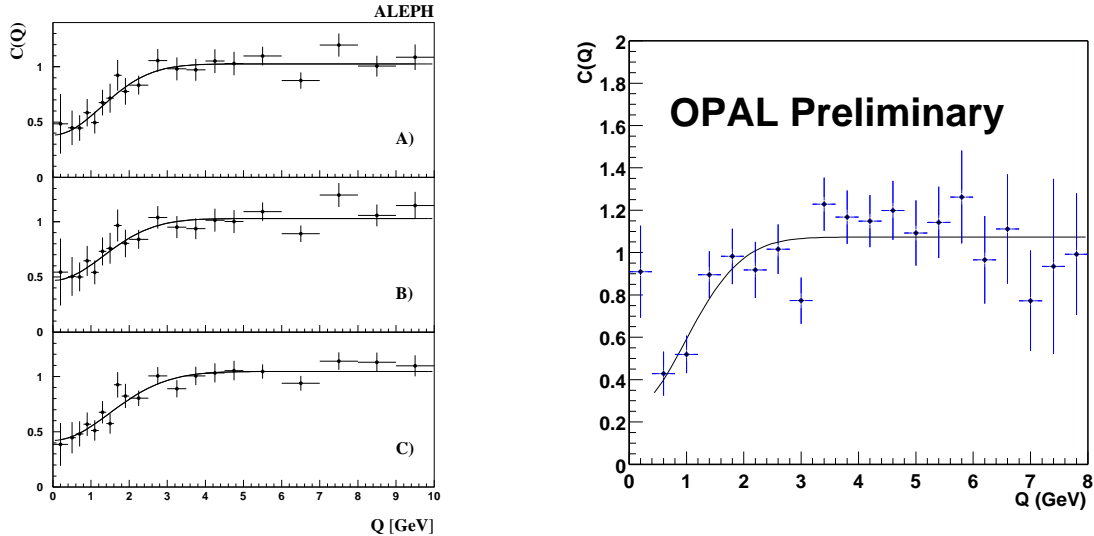


Figure 13: Left: The correlation function $C(Q)$ obtained by the ALEPH collaboration [100] using Method II for the $\Lambda\Lambda$ pairs for three different reference samples. A) Monte Carlo, B) and C) two, somewhat differently treated, mixed events samples. Right: The OPAL $C(Q)$ distribution of the $\bar{p}\bar{p}$ system taken from Ref. [101]. The continuous lines represent the best fit of Eq. (29) to the $C(Q)$ results.

Inserting this last expression for p in Eq. (41) one finally obtains

$$r(m) = \frac{\hbar c / \sqrt{\hbar / \Delta t}}{\sqrt{m}} = \frac{c\sqrt{\hbar\Delta t}}{\sqrt{m}}. \quad (44)$$

If one further assumes that Δt is independent of the hadron mass and its identity and just represents the time scale of strong interactions, of the order of $\Delta t = 10^{-24}$ seconds, then $r(m) = A/\sqrt{m}$ with $A = 0.243 \text{ fm GeV}^{1/2}$. This r dependence on m is shown in Fig. 14 by the thin solid line. The sensitivity of $r(m)$ to the value of Δt is represented by the dashed lines in the same figure. The upper and the lower dashed lines correspond respectively to the values of $\Delta t = 1.5 \times 10^{-24}$ and 0.5×10^{-24} seconds. A fit of Eq. (44) to the data points plotted in Fig. 14 yields $\Delta t = (1.2 \pm 0.3) \times 10^{-24}$ seconds where 0.3 represents the statistical error. As seen in the figure, the dependence of r on the mass m , as determined from the Heisenberg relations, follows within errors the measured values and thus offers a natural explanation for the experimental found hierarchy $r_{\pi\pi} > r_{KK} > r_{pp} \sim r_{\Lambda\Lambda}$.

6.2 QCD description of $r(m)$ via the virial theorem

In the previous section it has been shown that the observed hierarchy $\partial r / \partial m < 0$ has a natural and a rather general explanation. Here we would like to demonstrate that such a dependence could shed light on the character of the “soft” interaction or, in other words, on the non-perturbative QCD which is responsible for the interaction at long distances. In that we follow [102] and use the semi-classical approximation as in Sec. 6.1, which means that the angular momentum is given by

$$\ell = |\vec{p}_1 - \vec{p}_2| b_t = 2pb_t \approx \hbar c, \quad (45)$$

Table 4: Experimental results for r and λ extracted from Bose-Einstein and Fermi-Dirac correlations of boson and baryon-pairs present in the hadronic Z^0 decays produced in e^+e^- annihilations in the LEP1 collider.

h h	λ_2	r_2 [fm]	Experiment
$\pi^\pm \pi^\pm$	–	$0.78 \pm 0.01 \pm 0.16$	LEP1 Average [102]
$K^\pm K^\pm$	$0.82 \pm 0.11 \pm 0.25$	$0.48 \pm 0.04 \pm 0.07$	DELPHI [79]
	$0.82 \pm 0.22 \begin{smallmatrix} +0.17 \\ -0.12 \end{smallmatrix}$	$0.56 \pm 0.08 \begin{smallmatrix} +0.07 \\ -0.06 \end{smallmatrix}$	OPAL [80]
$K_S^0 K_S^0$	$1.14 \pm 0.23 \pm 0.32$	$0.76 \pm 0.10 \pm 0.11$	OPAL [103]
	$0.96 \pm 0.21 \pm 0.40$	$0.65 \pm 0.07 \pm 0.15$	ALEPH [104]
	$0.61 \pm 0.16 \pm 0.16$	$0.55 \pm 0.08 \pm 0.12$	DELPHI [79]
$\bar{p} \bar{p}$	–	$0.15 \pm 0.02 \pm 0.04$	OPAL [101]
$\Lambda \Lambda$	–	$0.11 \pm 0.02 \pm 0.01$	ALEPH [100]
$\Lambda \Lambda$	Spin Analysis	$0.19 \begin{smallmatrix} +0.37 \\ -0.07 \end{smallmatrix} \pm 0.02$	OPAL [98]
	“	$0.11 \begin{smallmatrix} +0.05 \\ -0.03 \end{smallmatrix} \pm 0.01$	DELPHI [99]
	“	$0.17 \pm 0.13 \pm 0.04$	ALEPH [100]

where b_t is the impact parameter. To estimate the value of p one uses the virial theorem [108] which provides a general connection between the average values of the kinetic and the potential energies (T and V), namely

$$2\langle T_t \rangle = \langle \vec{b}_t \cdot \vec{\nabla}_t V(r) \rangle, \quad (46)$$

where t denotes the transverse direction. Since the motion in the transverse direction is always finite, one can safely apply the virial theorem. Substituting in Eq. (46) the kinetic energy by its relation to the momentum, $T_t = p_t^2/m$, we obtain

$$\langle p_t^2 \rangle = m \langle \vec{r}_t \cdot \vec{\nabla}_t V(r) \rangle, \quad (47)$$

where r stands for the distance between the two particles with r_t being equal to $2b_t$.

From Eq. (47) follows that the relation between $\langle p^2 \rangle$ and r depends crucially on the r dependence of the potential energy $V(r)$. Here we take $V(r)$ to be independent of the interacting particles (quarks) mass. This assumption is based on the Local Parton Hadron Duality [109,110] concept, which states that one can consider the production of hadron as interaction of partons, i.e. gluons and quarks, in spite of the unknown mechanism of hadronisation. This approach is supported experimentally by the single and double inclusive hadron production in e^+e^- annihilation [109,110]. Since the interaction between partons is independent of the produced hadron mass it follows that $\partial V(r)/\partial m = 0$. Based on this assumption and using Eq. (45) and Eq. (46), one obtains an equation for the typical size of the emission volume, namely

$$r^2 \langle \vec{r} \cdot \vec{\nabla} V(r) \rangle \approx \frac{(\hbar c)^2}{m}. \quad (48)$$

Further one applies to Eq. (48) the general QCD potential

$$V(r) = \kappa r - \frac{4}{3} \frac{\alpha_S \hbar c}{r}, \quad (49)$$

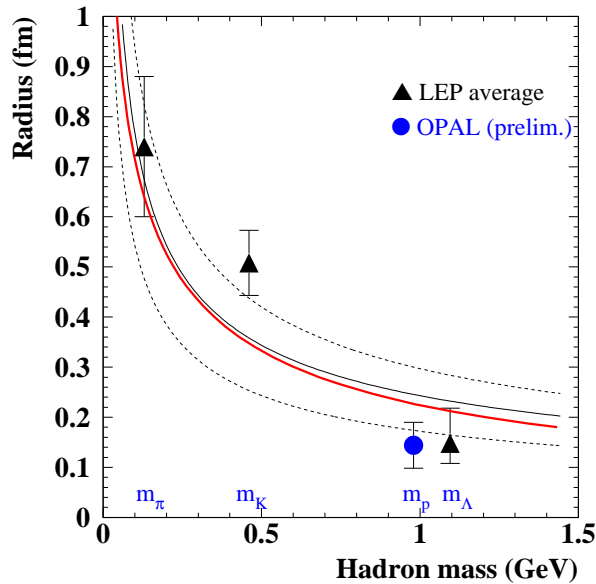


Figure 14: The dependence of r_2 on the hadron mass obtained from BEC and FDC analyses of identical hadron pairs emerging from the Z^0 decay. For clarity the data points are plotted at slightly displaced mass values. The error bars correspond to the statistical and systematic errors added in quadrature. The thin solid line represents the expectation from the Heisenberg uncertainty relations setting $\Delta t = 10^{-24}$ seconds [102]. The upper and the lower dashed lines correspond to $\Delta t = 1.5 \times 10^{-24}$ and 0.5×10^{-24} seconds respectively. The thick solid line represents the dependence of r_2 on the hadron mass as expected from a QCD potential given by Eq. (49).

widely used to derive the wave functions and decay constants of hadrons [111, 112]. Setting the potential parameters values to $\kappa = 0.14 \text{ GeV}^2 = 0.70 \text{ GeV/fm}$, $\alpha_s = 2\pi/9 \ln(\delta + \gamma/r)$ with $\delta = 2$ and $\gamma = 1.87 \text{ GeV}^{-1} = 0.37 \text{ fm}$ as derived from hadron wave functions and decay constants [111], the resulting dependence of r on the hadron mass, given by the solid thick line in Fig. 14, is seen to follow rather well the the data. Moreover, this QCD expectation essentially coincides with the prediction derived from the Heisenberg uncertainty relations (thin solid line in the same figure).

7 Results from multi-dimensional Bose-Einstein correlation analyses

The study of multi-dimensional BEC has gained considerable interest in recent years, in particular in heavy-ion collisions sector, but also in particle reactions. In the framework of the Lund hadronisation model it is expected that the emitter shape will deviate significantly from a sphere and that an elongation' of the source should occur. Three LEP experiments, in their study of the process $e^+e^- \rightarrow \gamma^*/Z^0 \rightarrow \text{hadrons}$, have analysed their data in the Longitudinal Centre-of-Mass System with the aim of extracting values for the longitudinal $r_z (= r_\ell)$, transverse r_T and side r_{side} dimensions (see Sec. 2.4). These are summarised in Table 5 together with the results from the ZEUS experiment at HERA ep collisions which confirm that the ratios r_{side}/r_z and r_T/r_z are significantly smaller than one. Missing however is a control experiment that will show that in the case of a genuine spherical emitter the multi-dimensional analysis

procedure will in fact yield the results that $r_{side}/r_z \approx r_T/r_z \approx 1$.

A somewhat surprising result which came out of the BEC multi-dimensional analysis of pion-pairs is the dependence of r_z , as well as r_{side} and r_T , on the transverse mass m_T . An example of this r_z dependence on m_T is the one reported by the DELPHI collaboration [113] which is shown in Fig. 15. This $r_z(m_T)$ behaviour is very similar to that seen in heavy ion collisions where it is often attributed to nuclei collective effects which should be absent in particle reactions and in particular in e^+e^- annihilations. A theoretical understanding in terms of the Lund model of this effect in particle reactions is apparently still lacking even if only for the reason that the inclusion of the BEC effect into the model is a highly non-trivial task and still seems to need further improvements [114,115].

Table 5: Evidence for the elongation of the source from experimental results for the ratios r_{side}/r_z and r_T/r_z obtained from multi-dimensional BEC analyses of identical charged pions. The first and the second errors are respectively the statistical and systematic ones.

Reaction	\sqrt{s} [GeV]	Experiment	r_{side}/r_z	r_T/r_z
$e^+e^- \rightarrow Z \rightarrow h$	91	L3 [37]	$0.80 \pm 0.02^{+0.03}_{-0.18}$	
$e^+e^- \rightarrow Z \rightarrow h$	91	OPAL [39]	$0.82 \pm 0.02^{+0.01}_{-0.05}$	
$e^+e^- \rightarrow Z \rightarrow h$	91	DELPHI [38]		$0.62 \pm 0.02 \pm 0.05$
$e p \rightarrow e h$	$110 < Q_\gamma^2$ [GeV ²]	ZEUS [16]		0.67 ± 0.08

7.1 $r_z(m_T)$ description in terms of the Heisenberg relations

We have seen that there is a great similarity between the dependence of the 1-dimensional r_2 on the hadron mass m and the dependence of the r_z on the transverse mass m_T . This is not surprising once one realises that the longitudinal distance Δr_z , and Δp_z , the difference in the longitudinal momentum of the two hadrons in the LCMS, are also conjugate observables which obey the uncertainty relation [116]

$$\Delta r_z \Delta p_z = \hbar c . \quad (50)$$

Here Δp_z is measured in GeV, $\Delta r_z \equiv r_z$ is given in Fermi units and $\hbar c = 0.197$ GeV fm. In the LCMS one has

$$\Delta p_z = 2\mu v_z = p_z ,$$

where $\mu = m/2$ is the reduced mass of the two identical hadrons of mass m and the longitudinal velocity v_z of these hadrons. Thus

$$r_z = \frac{\hbar c}{p_z} . \quad (51)$$

Simultaneously one considers the uncertainty relation expressed in terms of energy and time

$$\Delta E \Delta t = \hbar , \quad (52)$$

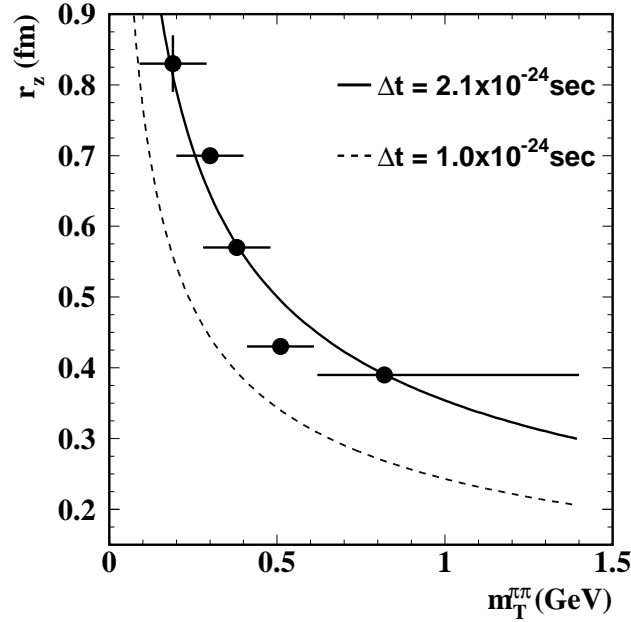


Figure 15: Preliminary results of DELPHI [113] for the dependence of the longitudinal emitter dimension $r_z(\pi\pi)$ on the transverse mass $m_T(\pi\pi)$ in hadronic Z^0 decays. The data are compared with the expression for r_z given in Eq. (59) setting Δt to the best fitted value of 2.1×10^{-24} sec (continuous line) and the expectation for 1.0×10^{-24} sec (dashed line).

where ΔE is given in GeV and Δt in seconds. In as much as the total energy E of the two-hadron system is given by their mass and their kinetic energy, i.e. the potential energy can be neglected, one has

$$E = \sum_{i=1}^2 \sqrt{m^2 + p_{i,x}^2 + p_{i,y}^2 + p_z^2} = \sum_{i=1}^2 \sqrt{m_{i,T}^2 + p_z^2}, \quad (53)$$

where $m_{1,T}$ and $m_{2,T}$ are the transverse mass of the first and second hadron. As Q_z decreases the longitudinal momentum p_z vanishes so that one can, once $p_z^2 < m_{i,T}^2$, expand the hadron energy E in terms of $p_z^2/m_{i,T}^2$ and retain only the two first terms,

$$E = \sum_{i=1}^2 m_{i,T} \sqrt{1 + \frac{p_z^2}{m_{i,T}^2}} \approx \sum_{i=1}^2 m_{i,T} + \sum_{i=1}^2 \frac{1}{2} \frac{p_z^2}{m_{i,T}}. \quad (54)$$

Next one can order the identical bosons so that $m_{1,T} \geq m_{2,T}$ and define

$$\delta m_T = \frac{m_{1,T} - m_{2,T}}{m_T^2 - (\delta m_T)^2} \quad \text{while} \quad m_T = \frac{m_{1,T} + m_{2,T}}{2}. \quad (55)$$

Inserting these relations into Eq. (54) one gets, after a few algebraic steps that

$$E = 2m_T + \frac{m_T p_z^2}{m_T^2 - (\delta m_T)^2}. \quad (56)$$

Thus as long as $m_T^2 \gg (\delta m_T)^2$ the total energy of the di-boson system is approximately equal to

$$E \approx 2m_T + \frac{p_z^2}{m_T}. \quad (57)$$

In the 2-dimensional analysis the r_z estimation is deduced from the BEC enhancement in the longitudinal direction, keeping m_T fixed and letting Q_z and therefore also p_z , approach zero. Thus as long as the uncertainty in $2m_T$ is much smaller than that of p_z^2/m_T one has

$$\Delta E \Delta t = \frac{p_z^2}{m_T} \Delta t = \hbar . \quad (58)$$

Combining Eqs. (51) and (58) one finally has

$$r_z(m_T) \approx \frac{c\sqrt{\hbar\Delta t}}{\sqrt{m_T}} . \quad (59)$$

This last equation is identical to the one given in Eq. (44) for the dependence of the emitter dimension on the boson mass when r and m are replaced by r_z and m_T . A fit of Eq. (59) to the data shown in Fig. 15 yields $\Delta t = (2.1 \pm 0.4) \times 10^{-24}$ sec so that $r_z(m_T) = 0.354/\sqrt{m_T}[\text{GeV}]$ fm. This Δt value is compatible with the corresponding value of $(1.2 \pm 0.3) \times 10^{-24}$ sec obtained in [102] from a fit to $r(m)$ in view of the considerable spread of the r values obtained from the 1-dimensional BEC analyses carried out with the LEP1 data. In heavy-ion collisions the longitudinal range r_z was also observed to be inversely proportional to the square root of m_T [12] namely, $r(m_T) \approx 2/\sqrt{m_T}[\text{GeV}]$ fm where the difference between the proportionality factor of 0.354 and 2.0 can be accounted for by the difference in the extent of the heavy ion targets as compared to that existing in the e^+e^- annihilation.

The dependence of the transverse dimension r_T on the two-pion transverse mass m_T has also been measured in the hadronic Z^0 decays [117]. Here again the transverse range was found to decrease as m_T increases. However unlike r_z which is a geometrical quantity, r_T is a mixture of the transverse radius and the emission time difference between the two hadrons so that a straightforward application of the uncertainty relations is improper.

7.2 Application of the Bjorken-Gottfried relation to $r(m_T)$

Another approach to account for the dependence of r_Z and r_T on the mass of the hadron has been taken in Refs. [118, 119]. In that approach the parameters characterising the particle emission region are mass independent and the observed change in radii is solely the consequence of the momentum-position correlation as expressed in the Bjorken-Gottfried condition [120–123]. In this hypothesis there exists a linear relation between the 4-momentum of the produced particle and the time-space position at which it is produced, namely

$$q_\mu = \lambda x_\mu \quad \text{which implies} \quad \lambda = m_T/\tau ,$$

where m_T is the transverse mass and $\tau = \sqrt{t^2 - z^2}$ is the longitudinal proper time after the collision. In the framework of this hypothesis relations between the longitudinal and transverse radii and the transverse mass can be derived. These are given in Fig. 16 by the dashed bands where they are seen to adequately describe the results obtained from the 1-dimensional BEC analyses carried out with the LEP1 data.

7.3 $r(m)$ and the interatomic separation in Bose condensates

The observation that the dimensions r and r_z derived from BEC analyses are seen respectively to be inversely proportional to \sqrt{m} and $\sqrt{m_T}$, naturally arouses the curiosity whether similar

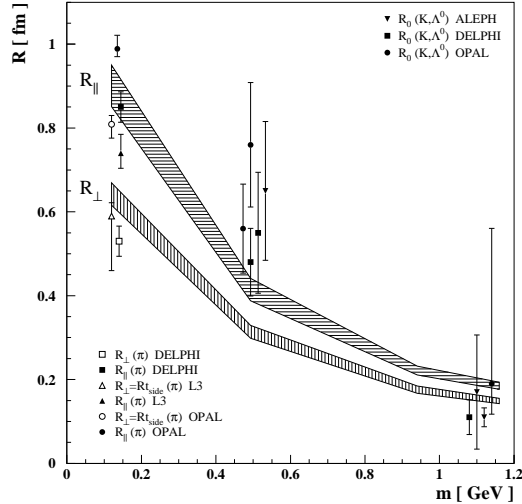


Figure 16: $r_z (=R_{||})$ and $r_T (=R_{\perp})$ as a function of the transverse mass m_T taken from Refs. [118,119]. The dashed bands were calculated from a model based on the Bjorken-Gottfried relation. The data points are taken from BEC analyses of hadronic Z^0 decays.

behaviour does also exist in other phenomena associated to the Bose-Einstein statistics. To this end we turn here to the Bose condensate states where we will show that the average interatomic separation is inversely proportional to the square-root of the atomic mass. In this presentation we follow closely reference [116] and first summarise briefly, for the benefit of the non-expert reader, the main features of the Bose condensates and focus on their interatomic separation.

When bosonic atoms are cooled down below a critical temperature T_B , the atomic wave-packets overlap and the equal identity of the particles becomes significant. At this temperature, these atoms undergo a quantum mechanical phase transition and form a Bose condensate, a coherent cloud of atoms all occupying the same quantum mechanical state. This phenomenon, first surmised by A. Einstein in 1924/5, is a consequence of quantum statistics [124, 125]. Detailed theoretical aspects of the Bose-Einstein condensation can be found in Ref. [126] and its recent experimental situation is described in Ref. [127]. Concise summaries, aimed in particular to the non-expert, both of the experimental aspects and the theoretical background, can be found in Refs. [128, 129]. To form Bose condensates, extremely dilute gases have to be cooled down below the critical temperature T_B , so that the formation time of molecules and clusters in three-body collisions is slowed down to seconds or even minutes to prevent the creation of the more familiar transitions into liquid or even solid states.

The existence of Bose-Einstein condensation was first demonstrated in 1995 by three groups [130–132] in cooling down rubidium, sodium and lithium. Typical temperatures where Bose condensates occur are in the range of 500 nK to 2 μ K with atom densities between 10^{14} and 10^{15} cm^{-3} . The largest sodium condensate has about 20 million atoms whereas hydrogen condensate can reach even one billion atoms.

Let us now consider a dilute homogeneous ideal gas of N identical bosonic atoms of spin zero confined in a volume V . These atoms occupy ϵ_i energy levels, handled here as a continuous variable, which are distributed according to the Bose-Einstein statistics. We further set the

ground state to be $\epsilon_0 = 0$. If N_0 is the number of atoms in this ground state and N_{ex} is the number of atoms in the excited states then $N = N_0 + N_{ex}$. For a homogeneous ideal gas of identical bosonic atoms it can be shown (see e.g. Ref. [133]) that at a low temperature T one has

$$N_{ex} = 2.612 V \left(\frac{2\pi mkT}{h^2} \right)^{3/2}, \quad (60)$$

where V is the volume occupied by the atoms of mass m . Since T_B is defined as the temperature where almost all bosons are still in excited states, we can, to a good approximation, equate N with N_{ex} . That is

$$N = 2.612 V \left(\frac{2\pi mkT_B}{h^2} \right)^{3/2}. \quad (61)$$

For $T < T_B$ one obtains from Eqs. (60) and (61) that the number of atoms N_0 which are in the condensate state is,

$$N_0 = N - N_{ex} = N \left[1 - \left(\frac{T}{T_B} \right)^{3/2} \right], \quad (62)$$

where T is the temperature of the atoms lying at the excited energy states above the condensate energy level $\epsilon_0 = 0$. The atomic density of the Bose gas at very low temperatures, $T/T_B \ll 1$ where $N \approx N_0$, is then given by

$$\rho = \frac{N}{V} = 2.612 \left(\frac{2\pi mkT}{h^2} \right)^{3/2}, \quad (63)$$

where k is the Boltzmann constant and ρ , the atomic density, has the dimension of L^{-3} . From this follows that $\rho^{-1/3}$ is the average interatomic separation in the Bose condensate. At the same time the thermal de Broglie wave length is equal to

$$\lambda_{dB} = \left(\frac{h^2}{2\pi mkT} \right)^{1/2}. \quad (64)$$

Combining Eqs. (63) and (64) one has for the state of a Bose condensate the relation

$$\rho \lambda_{dB}^3 \approx 2.612. \quad (65)$$

Thus the average interatomic distance in a Bose condensate, d_{BE} , is equal to

$$d_{BE} \equiv \rho^{-1/3} \approx \lambda_{dB}/1.378. \quad (66)$$

Next one can consider two different bosonic gases, having atoms with masses m_1 and m_2 , which are cooled down to the same very low temperature T_0 , below the critical temperature T_B of both of them. In this case one produces two Bose condensates with interatomic distances

$$d_{BE}(m_i) \approx \frac{\sqrt{2\pi}}{1.378} \left(\frac{\hbar^2}{m_i k T_0} \right)^{1/2}; \quad i = 1, 2. \quad (67)$$

From this follows that when two condensates are at the same fixed temperature T_0 one has

$$\frac{d_{BE}(m_1)}{d_{BE}(m_2)} = \sqrt{\frac{m_2}{m_1}}, \quad (68)$$

which is also the expectation of Eq. (44) for the r dependence on the mass of the hadron produced in high energy reactions provided Δt is fixed. Finally it is interesting to note that in as much as one is justified, since almost all the atoms occupy the same quantum mechanical state, to replace in Eq. (67), at very low temperatures, kT_0 by ΔE and use the uncertainty relation $\Delta E = \hbar/\Delta t$ one derives the expression for $r(m)$ as given by Eq. (44) multiplied by the factor $\sqrt{2\pi}/1.378$. Thus in Bose-Einstein condensates $r(m)$ measures the interatomic separation and not the dimension of the condensate ensemble, a deduction which will be further referred to in Sec. 8.

In relating the condensates to the production of hadrons in high energy reactions one should keep in mind that the interatomic separation proportionality to $1/\sqrt{m_{atom}}$ does not necessarily imply that it should also apply to hadrons produced in high energy reactions. Common to both systems is their bosonic nature which allows all hadrons (atoms) to occupy the same lowest energy state. In addition the condensates are taken to be in a thermal equilibrium state. Among the various models proposed for the production of hadrons in high energy e^+e^- and nucleon-nucleon reactions some attempts have also been made to explore the application of a statistical thermal-like model [134]. Whether this approach will eventually prevail is at present questionable. Finally the condensates are taken to be in a coherent state. In the case of hadrons one is able to measure r via BEC only if the chaoticity factor λ in Eq. (9) is different from zero i.e., only if the source is not 100% coherent. However so far there is no evidence from BEC studies in hadron production for a dependence of r on λ apart from that introduced by the correlated errors between Δr and $\Delta \lambda$ produced by fitting Eq. (9) to the data.

8 On the relation between r and the emitter size

As it has been pointed out in the introduction, the HBT interferometry in astronomy and its equivalent, the GGLP correlations in its application to heavy ion collisions, have been rather successful in estimating respectively the dimensions and configurations of stellar objects and the geometrical extent of nuclei. In the elementary particle sector it looks as if the r dimension is very little if at all dependent on the type and energy of the reaction. Furthermore e^+e^- annihilations, there seem to be several features which pose a challenge to the general belief that r measures a quantity which represents the emitter volume and corresponds to its radius in the spherical approximation.

In the Lund string model one expects that the extension of the emitter of hadrons in elementary particle reactions will increase with multiplicity and hence with energy and certainly in e^+e^- annihilation at 91 GeV will spread over more than several fm. From the Bose-Einstein correlation analyses there is no evidence for such a behaviour. In fact, the r values obtained from $\pi^\pm\pi^\pm$ pairs produced in e^+e^- annihilation seem to be rather independent of energy having values in the vicinity of 0.75 fm (see Table 1).

Moreover, recent experimental results show that the dimension r , measured in e^+e^- annihilations on the Z^0 mass energy, does depend on the hadron mass. As shown in Sec. 6, the r values at the proton and Λ masses decrease to the very low value of ~ 0.15 fm as compared to approximately 0.75 fm for pions and kaons. This behaviour of $r(m)$ is very similar to the interatomic separation dependence on the atomic mass in equal temperature Bose condensates. In as much as one is justified to infer from the Bose condensates features to the hadron pro-

duction sector, $r(m)$ apparently does not measure the emitter radius but rather the distance between two neighbouring identical hadrons.

In any case, the experimental results found for the dependence of r on the hadron mass are not reconcilable with the notion of a unique emitter radius for all outgoing hadrons. However the possibility that baryons are emitted from a much smaller source than pions and kaons has its own difficulty [135] if one considers the source energy density ϵ . To illustrate this problem let us assume that the emitter source is a sphere of radius r , as determined from the correlation analysis, filled homogeneously with at least the energy which corresponds to the sum of the rest masses of the two outgoing identical hadrons. Then, for a given hadron mass m_h and its emitter radius r_h , the energy density of the source is given by

$$\epsilon_{measured} = \frac{3}{4\pi} \frac{2m_h}{r_h^3} \quad (69)$$

which is plotted in Fig. 17 for the pion, kaon, proton and Λ pairs. The dashed lines in the figure are the predicted dependence of the energy density on the hadron mass computed from Eq. (70), which is based on the expression of $r(m)$ given in Eq. 44, namely

$$\epsilon_{model} = \frac{3}{2\pi} \frac{m_h^{5/2}}{c^3 (\hbar \Delta t)^{3/2}} \quad (70)$$

Whereas the energy density of the pion and kaon pairs are still lying within an acceptable range, the energy density of the proton and Λ emitter sources reach the very high value of about 100 GeV/fm³.

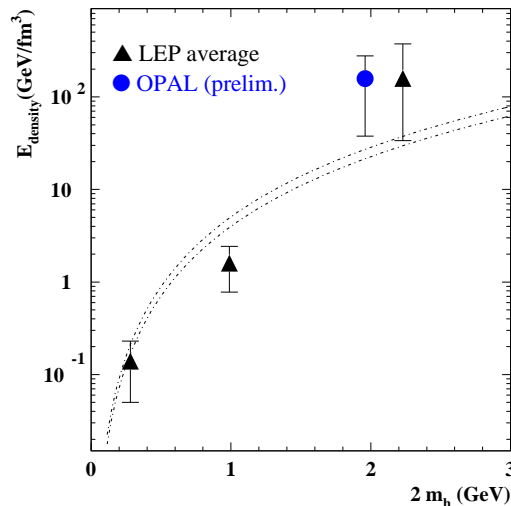


Figure 17: Energy density of the hadron emitter, calculated from Eq. (69), as a function of the hadron mass assuming a spherical emitter having the radius r which was extracted from the BEC analysis. The dashed lines are the expectations from Eq. (70) setting Δt to plus and minus three standard deviations away from its median value of 1.2×10^{-24} seconds [135].

In trying to cope with these observations, it may be helpful to try and identify the underlying variable or variables, apart from the hadron mass, which r depends on. A partial

answer to this quest [136], which is briefly outlined in the following section, is provided by the relation between the BEC analysis and the genuine particle correlation method which utilises the factorial cumulant moments (see Sec. 2.3).

8.1 The r dependence on the number of emitting sources

Let us consider a simplified description of heavy ions (AA) interactions at high energies which is given in terms of several distinct, say S , primary nucleon-nucleon (nn) collisions leading to hadrons. In this approach the hadrons produced in a single primary nucleon-nucleon reaction are emitted from an S_{nn} source. The hadron produced in heavy ion (AA) collisions are then coming from S_{AA} sources so that $S_{AA}/S_{nn}=S$. Since here the AA collisions are described in terms of the single primary nucleon-nucleon reactions one can define, without loss of generality, S_{nn} as a unit source so that $S_{AA} = S$.

Next the $\pi^\pm\pi^\pm$ pairs emerging from a single primary nucleon-nucleon reaction and those emerging from the heavy ion collisions are subject to BEC analyses and the correlation functions

$$C_2^{S=1}(Q) = 1 + \lambda_{S=1}e^{-Q^2r_{S=1}^2} \quad \text{and} \quad C_2^S(Q) = 1 + \lambda_S e^{-Q^2r_S^2}$$

are fitted, each to its corresponding data distribution. In general for every S value the resulting r_S can be extracted from the fitted correlation functions by integration $C_2 - 1$ over Q from zero to infinity so that

$$\int_0^\infty [C_2^S(Q) - 1] dQ = \int_0^\infty \lambda_S e^{-Q^2r_S^2} dQ = \frac{1}{2} \frac{\lambda_S \sqrt{\pi}}{r_S}, \quad (71)$$

where λ_S is, as customary in the BEC analyses, taken to be independent of Q .

For the two-particle correlation there exists a relation (see e.g. Ref. [137]) between the cumulant K_2 and the BEC function C_2 , namely that

$$C_2(Q) = 1 + \lambda e^{-r^2Q^2} = 1 + K_2. \quad (72)$$

In addition it has been shown [138–140] that for two particle correlation the cumulant K_2^S of S sources is, to a very good approximation, related to the value of the corresponding cumulant of one source, $K_2^{S=1}$, by

$$K_2^S = K_2^{S=1}/S.$$

Thus the BEC function C_2^S is equal to

$$C_2^S(Q) = 1 + \lambda_S e^{-r_S^2 Q^2} = 1 + \frac{K_2^{S=1}}{S} = 1 + \frac{\lambda_{S=1} e^{-r_{S=1}^2 Q^2}}{S}. \quad (73)$$

By integrating Eq. (73) over Q from zero to infinity one finally obtains that

$$r_S = S \frac{\lambda_S}{\lambda_{S=1}} r_{S=1}, \quad (74)$$

where S like the λ parameters is taken to be independent of Q . Consequently if the increase of an emitter volume is coupled to an increase in the number of boson sources, then the BEC extracted r_S will grow as well. Further to note is that if in heavy-ion collisions $S\lambda_S/\lambda_{S=1}$ is

proportional to $A^{1/3}$ then r will be proportional to the nucleus radius. As for the HBT analysis applied in astronomy, the proportionality between the stellar object dimension and the number of photon sources is self-evident.

From the discussion above it is obvious that the choice of the unit source determines the predicted dependence of r on the various features, such as type and energy, of the hadron (or photon) emitting reaction. In the case of heavy ion collisions the choice of the unit source to be a single primary nucleon-nucleon collision is a natural one. In the case of e^+e^- annihilation one may consider the possibility that S_{ee} itself is the unit source. Under this assumption the number of sources does not change with energy and r will remain constant. This prediction seems to be consistent with the measured r values allowing for the fact that the various experiments used different analysis methods and reference samples (see Sec. 5.1). On the other hand an increase of r as a function of the hadron multiplicity has been observed in the BEC analysis [22] of equally non-zero charged pion-pairs emerging from the Z^0 decay. Furthermore the same experiment also found that the extracted r value from the Z^0 decays into three hadron jets was by about 10% higher than that obtained from the Z^0 decay events having only two hadron jets. Similar rise of r with the average hadron multiplicity has also been reported by several hadron-hadron collision experiments carried out at centre of mass energies above 30 GeV [73, 141–143].

These last findings indicate that apparently for the e^+e^- annihilations a reasonable choice for the unit source is the single hadron jet. The shortcoming of such a choice is however the fact that the charge multiplicity of a hadron jet depends on its energy and on its origin, i.e. if it is a quark or a gluon [144–146], which currently impedes a detailed quantitative prediction for the behaviour of r as a function of the centre of mass energy and the multiplicity. Regardless of these hindrances, the adaptation of the hadron jet as a unit source provides nevertheless a qualitative explanation for the increase of r with multiplicity and also expects in e^+e^- annihilations a moderate dependence of r on the e^+e^- centre of mass energy.

9 Summary and conclusions

The 1-dimensional Bose-Einstein correlation enhancement measured in identical pion-pairs close in time-phase space, is found to be a universal phenomenon present in a large variety of particle reactions and over a wide range of energies. Nevertheless, there are still missing systematic BEC studies concentrating on the same reaction at different energies, and/or different reactions at the same energy, which will allow a comprehensive investigation of the dependence of r on the variables that characterise the particle interactions. Notwithstanding the fact that these systematic studies are still missing and that BEC analyses cannot currently be considered as precision measurements, the extracted r values, which are taken to represent the hadron emitter source, seem to be very little, if at all, dependent on the reaction type or on its energy and they are seen to fluctuate in the range of about 0.6 to 1.0 fm.

The essentially constant r value seems to be in contradiction with the results obtained from the BEC studies of heavy-ion collisions and from the HBT analyses of stellar objects. An insight into the origin of this difference is offered by the relation between the BEC and the cumulant moments analysis where the introduction of the so called hadron source plays a

central role. From this relation follows that the value of r is proportional to the number of active hadron sources which participate in the reaction. In particle reactions the proposal to equate the number of sources with the number of hadron jets offers an understanding of the r dependence on multiplicity. At the same time however the difficulty in defining a standard hadron jet prohibits presently any quantitative results.

The genuine higher order BEC analyses are presently restricted to three identical charged pions. Assuming a Gaussian hadron emitter, the expected relation $r_2/\sqrt{3} \leq r_3 \leq r_2/\sqrt{2}$ between the two and three-pion BEC dimension parameters, is found to be consistent within errors with the measurements carried out in e^+e^- annihilation and hadron collisions. The direct measurement of the genuine correlations of four and more pion systems has not been realised so far. On the other hand the extracted r values from the , so to speak, non-genuine correlations, are model dependent and as such less reliable.

Recently first results from 2 and 3-dimensional BEC analyses of pion-pairs have been reported. These verified the Lund string model expectation that the hadron emitter source deviates from a sphere and is elongated in the thrust (or sphericity) direction of the multi-hadron final state. In the approximation that the emitter has an elongated prolate ellipsoid shape, where the long axis r_ℓ is in the thrust direction and r_T is the axis perpendicular to it, the ratio r_T/r_ℓ is found to be in the range of ~ 0.7 to ~ 0.8 .

The extension of the BEC analysis to the fermion sector was shown to be feasible via the Pauli exclusion principle. First results from the so called Fermi-Dirac correlation analysis of the $\Lambda\Lambda$ and proton-proton pairs, emerging from the hadronic Z^0 decays, have demonstrated that the dimension r is strongly dependent on the mass of the identical hadrons. It has been further shown that this dependence can be accounted for by the Heisenberg uncertainty relations, or alternatively by QCD derived potential, to yield the relation $r(m) \propto 1/\sqrt{m}$. Similar relation is seen to be valid also in the 2-dimensional BEC analysis when r is replaced by the r_ℓ and m by the transverse mass m_t . It is interesting further to note that the interatomic separation in the Bose condensates having the same low temperature, is proportional to $1/\sqrt{m_{atom}}$.

So far the FDC analyses were restricted to the Z^0 hadronic decays, therefore it is essential that they will be repeated in other particle reactions to verify that indeed r of the Λ and the proton pairs is in the vicinity of 0.15 fm. This small r value, derived from the FDC analyses of baryon-pairs, poses a challenge to the concept that r represents the hadron emitter radius. If one does insist on keeping the radius emitter interpretation for r then one encounters the situation of an unreasonable high energy density value, of some 100 GeV/fm³, of the baryons source. Thus the very small $r_{\Lambda\Lambda}$ and r_{pp} values indicate that our level of understanding the production of hadrons, and in particular baryons, is apparently far from being satisfactory.

Acknowledgements

I would like to express my thanks to my colleagues G. Bella, I. Cohen, E.K. Grinbaum-Sarkisyan, P. Söding, and E. Tsur for many helpful discussions and comments. I am in particular indebted to B. Ilan for going diligently over the manuscript to ensure that it is free of errors and omissions.

References

- [1] R. Hanbury-Brown and R. Q. Twiss. *Phil. Mag.*, 45:663, 1954.
- [2] R. Hanbury-Brown and R. Q. Twiss. *Nature*, 177:27, 1956.
- [3] R. Hanbury-Brown and R. Q. Twiss. *Nature*, 178:1046, 1956.
- [4] D. H. Boal, C. K. Gelbke, and B. K. Jennings. *Rev. Mod. Phys.*, 62:553, 1990.
- [5] G. Baym. *Acta Phys. Polon.*, B29:1839, 1998.
- [6] U. A. Wiedemann and U. Heinz. *Phys. Rept.*, 319:145, 1999.
- [7] G. Goldhaber et al. *Phys. Rev. Lett.*, 3:181, 1959.
- [8] G. Goldhaber et al. *Phys. Rev. Lett.*, 120:300, 1960.
- [9] G. Alexander and H. J. Lipkin. *Phys. Lett.*, B352:162, 1995.
- [10] A. D. Chacon et al. *Phys. Rev.*, C43:2670, 1991, and references therein.
- [11] U. Heinz. Hanbury-Brown Twiss interferometry for relativistic heavy ion collisions: theoretical aspects. In *Proc. of Int. Summer School on Correlations and Clustering Phenomena in Subatomic Physics*, page 137, Dronnten, The Netherlands, 1996.
- [12] U. Heinz and B.V. Jacak. *Ann. Rev. Nucl. Part. Sci.*, 49:529, 1999, and references therein.
- [13] R. M. Weiner. *Phys. Rept.*, 327:249, 2000.
- [14] M. Ringnér. *Correlations in multiparticle production*. PhD thesis, Lund University, Lund, Sweden, 1998.
- [15] OPAL collaboration, P. D. Acton, et al. *Phys. Lett.*, B267:143, 1991.
- [16] ZEUS collaboration, M. Derrick. *Acta Phys. Polon.*, B33:3281, 2002.
- [17] T. Osada, S. Sano, and M. Biyajima. *Z. Phys.*, C72:285, 1996.
- [18] G. I. Kopylov and M. I. Podgoretskii. *Sov. J. Nucl. Phys.*, 15:219, 1972.
- [19] G. I. Kopylov and M. I. Podgoretskii. *Sov. J. Nucl. Phys.*, 18:336, 1973.
- [20] G. I. Kopylov. *Phys. Lett.*, B50:472, 1974.
- [21] W Hofmann. A fresh look at Bose-Einstein correlations. Research Note LBL-23108, Lawrence Berkeley Laboratory, UC, 1987.
- [22] OPAL collaboration, G. Alexander, et al. *Z. Phys.*, C72:389, 1996.
- [23] E. A. De Wolf, I. M. Dremin, and W. Kittel. *Phys. Rept.*, 270:1, 1996.
- [24] MARK II collaboration, I. Juricic, et al. *Phys. Rev.*, D39:1, 1989.
- [25] M. Biyajima et al. *Prog. Theor. Phys.*, 84:931, 1990.

- [26] UA1-MINIMUM BIAS collaboration, N. Neumeister, et al. *Phys. Lett.*, B275:186, 1992.
- [27] P. Carruthers and I. Sarcevic. *Phys. Rev. Lett.*, 63:1562, 1989.
- [28] E. A. De Wolf. *Acta Phys. Pol.*, B21:611, 1990.
- [29] R. J. Barlow. *Statistics*. John Wiley & Sons., 1989.
- [30] T. Csörgö and S. Pratt. Structure of the peak in Bose-Einstein correlation. In T. Csörgö et al., editors, *Proc. of the Workshop on relativistic heavy ion physics*, page 75, Budapest, Hungary, 17-21 June 1991.
- [31] K. Geiger et al. *Phys. Rev.*, D61:054002, 2000.
- [32] DELPHI collaboration, P. Abreu, et al. *Phys. Lett.*, B471:460, 2000.
- [33] NA44 collaboration, H. Beker, et al. *Phys. Rev. Lett.*, 74:3340, 1995.
- [34] NA35 collaboration, T. Alber, et al. *Z. Phys.*, C66:77, 1995.
- [35] EHS/NA22 collaboration, N. M. Agababyan, et al. *Z. Phys.*, C66:409, 1995.
- [36] EHS/NA22 collaboration, N. M. Agababyan, et al. *Z. Phys.*, C71:405, 1996.
- [37] L3 collaboration, M. Acciarri, et al. *Phys. Lett.*, B458:517, 1999.
- [38] DELPHI collaboration, P. Abreu, et al. *Phys. Lett.*, B471:460, 2000.
- [39] OPAL collaboration, G. Abbiendi, et al. *Eur. Phys. J.*, C16:423, 2000.
- [40] B. Andersson and M. Ringnér. *Nucl. Phys.*, B513:627, 1998.
- [41] B. Andersson and M. Ringnér. *Phys. Lett.*, B421:283, 1998.
- [42] E. Segrè. *Nuclei and Particles*. Benjamin/Cummings Publishing Co., 2nd edition, 1982.
- [43] Particle Data Group, K. Hagiwara, et al. *Phys. Rev.*, D66:1, 2002.
- [44] E. P. Wigner. *Z. Phys.*, 43:624, 1927.
- [45] C. Eckart. *Rev. Mod. Phys.*, 2:305, 1930.
- [46] R. Lednicky. On correlation and spin composition techniques. Research Note PhE-10, MPI, 1999.
- [47] B. Andersson et al. *Phys. Rep.*, 97:31, 1983.
- [48] B. R. Webber. *Nucl. Phys.*, B238:492, 1984.
- [49] B. Andersson and M. Ringnér. *Nucl. Phys.*, B513:627, 1998.
- [50] M. Gyulassy et al. *Phys. Rev.*, C20:2267, 1979.
- [51] M. G. Bowler. *Phys. Lett.*, B270:69, 1991.
- [52] M. Biyajima et al. *Phys. Lett.*, B353:340, 1995.

- [53] E. Tsur. Bose-Einstein correlations of three charged pions in hadronic Z^0 decays. Master's thesis, Tel-Aviv University, Tel-Aviv, Israel, 1997.
- [54] Y. M. Liu et al. *Phys. Rev.*, C34:1667, 1986.
- [55] J. G. Cramer. *Phys. Rev.*, C43:2798, 1991.
- [56] E. O. Alt et al. *Eur. Phys. J.*, C13:663, 2000.
- [57] TPC collaboration, H. Aihara, et al. *Phys. Rev.*, D31:996, 1985.
- [58] TASSO collaboration, M. Althoff, et al. *Z. Phys.*, C30:355, 1986.
- [59] AMY collaboration, S. K. Choi, et al. *Phys. Lett.*, D355:406, 1995.
- [60] ALEPH collaboration, D. Decamp, et al. *Z. Phys.*, C54:75, 1992.
- [61] DELPHI collaboration, P. Abreu, et al. *Phys. Lett.*, B286:201, 1992.
- [62] L3 collaboration, P. Achard, et al. *Phys. Lett.*, B524:55, 2002.
- [63] M. Sanders. *Pion (non-) correlations in hadronic events at the Z resonance*. PhD thesis, The Nijmegen Catholic University, The Netherlands, 2002.
- [64] OPAL Collaboration, Physics Note PN-513, 2002. Submitted to the XXXII Int. Symp. on Multiparticle Dynamics (ISMD), 7-13 September 2002, Alushta, Ukraine.
- [65] CELLO collaboration, H. J. Behrend, et al. *Phys. Lett.*, B245:298, 1990.
- [66] Big Bubble Chamber Neutrino collaboration, V. A. Korotkov, et al. *Z. Phys.*, C60:37, 1993.
- [67] EMC collaboration, M. Arneodo et al. *Z. Phys.*, C32:1, 1986.
- [68] NA22 collaboration, M. Adamus, et a. *Z. Phys.*, C37:347, 1988.
- [69] NA23 collaboration, J. L. Bailly, et al. *Z. Phys.*, C43:431, 1989.
- [70] NA27 collaboration, M. Aguilar-Benitez, et al. *Z. Phys.*, C54:21, 1992.
- [71] AFS collaboration, T. Åkesson, et al. *Z. Phys.*, C36:517, 1987.
- [72] CPLEAR collaboration, R. Adler, et al. *Z. Phys.*, C63:541, 1994.
- [73] UA1 collaboration, C. Albajar, et al. *Phys. Lett.*, B226:410, 1989.
- [74] H1 collaboration, C. Adloff, et al. *Z. Phys.*, C75:437, 1997.
- [75] The LEP collaborations, ALEPH, DELPHI, L3, OPAL, and the LEP WW working group. CERN EP preprint, 2003.
- [76] DELPHI collaboration, N. van Remortel, et al. In *Proc. of Int. Symp. on Multiparticle Dynamics*, Alushta, Ukraine, 7-13 September 2002.
- [77] L3 collaboration, P. Achard, et al. *Phys. Lett.*, B547:139, 2002.

- [78] ALEPH collaboration, R. Barate, et al. *Phys. Lett.*, B478:50, 2000.
- [79] DELPHI collaboration, P. Abreu, et al. *Phys. Lett.*, B379:330, 1996.
- [80] OPAL collaboration, G. Abbiendi, et al. *Euro. Phys. J.*, C21:23, 2001.
- [81] H. J. Lipkin. *Phys. Lett.*, B219:474, 1989.
- [82] H. J. Lipkin, Argonne National Laboratory priprint ANL-HEP-PR-88-66, 1988.
- [83] H. J. Lipkin. *Phys. Rev. Lett.*, 69:3700, 1992.
- [84] G. Alexander. Bose-Einstein effect in the $K^0 \bar{K}^0$ in boson-antiboson system. Research Note 93/001, LNF, 1993.
- [85] DELPHI collaboration, P. Abreu, et al. *Phys. Lett.*, B298:236, 1993.
- [86] G. Alexander and H. J. Lipkin. *Phys. Lett.*, B456:270, 1999.
- [87] M. Biyajima et al. *Phys. Rev.*, C58:2316, 1998.
- [88] M. Suzuki. *Phys. Rev.*, D35:3359, 1987.
- [89] M. G. Bowler. *Phys. Lett.*, B197:443, 1987.
- [90] D. Morgan and M. R. Pennington. *Phys. Lett.*, B258:44, 1991.
- [91] D. Morgan and M. R. Pennington. *Phys. Rev.*, D48:1185, 1993.
- [92] F. E. Close et al. *Phys. Lett.*, B319:291, 1993.
- [93] DELPHI collaboration, P. Abreu, et al. *Phys. Lett.*, B355:415, 1995.
- [94] OPAL collaboration, K. Ackerstaff, et al. *Eur. Phys. J.*, C5:239, 1998.
- [95] L3 collaboration, P. Achard, et al. *Phys. Lett.*, B540:185, 2002.
- [96] EHS/NA22 collaboration, N. M. Agababian, et al. *Z. Phys.*, C68:229, 1995.
- [97] NA23 collaboration, J. L. Baily, et al. *Z. Physik*, C43:341, 1989.
- [98] OPAL collaboration, G. Alexander, et al. *Phys. Lett.*, B384:377, 1996.
- [99] DELPHI collaboration, T. Lesiak and H. Palka. Determination of the spin composition of $\Lambda\bar{\Lambda}$ and $\Lambda\Lambda$ ($\bar{\Lambda}\bar{\Lambda}$) pairs in hadronic Z decays (DELPHI 98-114 CONF 176). In *Proc. of the XXIX Int. Conf. on High Energy Physics*, Vancouver, Canada, 22-29 July 1998.
- [100] ALEPH collaboration, R. Barate, et al. *Phys. Lett.*, B475:395, 2000.
- [101] OPAL Collaboration, Physics Note PN486, 2002. Submitted to the Int. Conf. on High Energy Physics (HEP 2001) 12-18 July 2001, Budapest, Hungary.
- [102] G. Alexander, I. Cohen, and E. Levin. *Phys. Lett.*, B452:159, 1999.
- [103] OPAL collaboration, R. Akers, et al. *Z. Phys.*, C67:389, 1995.

- [104] ALEPH collaboration, D. Buskulic, et al. *Z. Phys.*, C64:361, 1994.
- [105] SELEX collaboration, I. Eschrich, et al. *Phys. Lett.*, B522:233, 2001.
- [106] M. Smith. *Phys. Lett.*, B477:141, 2000.
- [107] B. Andersson. Some theory remarks on Bose-Einstein correlation. In *Proc. of the XXVth Les Rencontres de Moriond*, Les Arcs, France, 18-20 March 2000.
- [108] C. Cohen-Tannoudji, B. Diu, and F. Lalöe. *Quantum Mechanics*. John Wiley and Sons publishing Co., 1990.
- [109] Ya. Asimov et al. *Z. Phys.*, C31:213, 1986, and references therein.
- [110] V. A. Khoze and W. Ochs. *Int. J. Mod. Phys.*, A12:2949, 1997, and references therein.
- [111] M. R. Ahmady, R. R. Mendel, and J. D. Talman. *Phys. Rev.*, D55:419, 1997, and references therein.
- [112] B. Blok and M. Lublinsky. *Phys. Rev.*, D57:2676, 1998, and references therein.
- [113] B. Lörstad and O.G. Smirnova. Transverse mass dependence of Bose-Einstein correlation radii in e^+e^- annihilation at LEP energies. In *Proc. 7th Int. Workshop on Multiparticle Production: Correlations and Fluctuations*, page 42, Nijmegen, The Netherland, 1997. World Scientific Publishing Co.
- [114] O. Smirnova. *Nucl. Phys. (Proc. Suppl.)*, B92:301, 2001.
- [115] S. Todorova-Nova. Bose-Einstein correlations at LEP and HERA. In *Proc. of the XXXI Int. Conf. on High Energy Physics*, Amsterdam, 24-31 July 2002.
- [116] G. Alexander. *Phys. Lett.*, B506:45, 2001.
- [117] L3 collaboration,. Study of Bose-Einstein correlations in Z decays at LEP. In *Proc. XXIX Int. Conf. on HEP*, Vancouver, 1998.
- [118] A. Bialas et al. *Phys. Rev.*, D62:114007, 2000.
- [119] A. Bialas et al. *Acta Phys. Polon.*, B32:2901, 2001.
- [120] K. Gottfried. *Phys. Rev. Lett.*, 32:957, 1974.
- [121] F. E. Low and K. Gottfried. *Phys. Rev.*, D17:2487, 1978.
- [122] J. D. Bjorken. *Phys. Rev.*, D27:140, 1983.
- [123] J. D. Bjorken. *Phys. Rev.*, D7:282, 1973.
- [124] A. Einstein. Sitzber. Kgl. Preuss. Akad. Wiss. rep. 261, 1924.
- [125] A. Einstein. Sitzber. Kgl. Preuss. Akad. Wiss. rep. 3, 1925.
- [126] F. Dalfovo et al. *Rev. Mod. Phys.*, 71:463, 1999, and references therein.

- [127] See e.g. the Georgia Southern University BEC bibliography on the web at [http:// amo.phy.gasou.edu/bec.html/bibliography.html](http://amo.phy.gasou.edu/bec.html/bibliography.html).
- [128] W. Ketterle. *Physics Today*, 52(12):30, 1999.
- [129] K. Burnett, M. Edwards, and C. Clark. *Physics Today*, 52(12):37, 1999.
- [130] M. H. Anderson et al. *Science*, 269:198, 1995.
- [131] K. B. Davis et al. *Phys. Rev. Lett.*, 75:3969, 1995.
- [132] C. C. Bradley et al. *Phys. Rev. Lett.*, 75:1687, 1995.
- [133] D. H. Trevena. *Statistical Mechanics – An Introduction*. Prentice-Hall/Ellis Horwood, 1993.
- [134] F. Becattini, L. Bellucci, and G. Passaleva. Transverse momentum spectra of identified particles in high energy collisions with statistical hadronisation model. In A. Giovannini and R. Ugoccioni, editors, *Proc. IX Int. Workshop on Multiparticle Production*, page 363, Torino, Italy, 12-17 June 2000, and references therein. *Nucl. Phys. B (Suppl.)* 92 (2001) 363.
- [135] G. Alexander, *Emitter size as a function of mass and transverse mass*, hep-ph/0108194, In Proceedings of the EPS International Conference on High Energy Physics, Budapest, 2001 (D. Horvath, P. Levai, A. Patkos, eds.), JHEP (<http://jhep.sissa.it/>), Proceedings Section, PrHEP-hep2001/027.
- [136] G. Alexander and E. K. G. Sarkisyan. To be published.
- [137] J. G. Cramer and K. Kadija. *Phys. Rev.*, C53:908, 1996.
- [138] P. Lipa and B. Bushbeck. *Phys. Lett.*, B223:465, 1989.
- [139] B. Bushbeck, H. C. Eggers, and P. Lipa. *Phys. Lett.*, B481:187, 2000.
- [140] G. Alexander and E. K. G. Sarkisyan. *Phys. Lett.*, B487:215, 2000.
- [141] AFS collaboration, T. Åkesson, et al. *Phys. Lett.*, B129:269, 1983.
- [142] AFS collaboration, T. Åkesson, et al. *Phys. Lett.*, B187:420, 1987.
- [143] SFM collaboration, A. Breakstone, et al. *Z. Phys.*, C33:333, 1987.
- [144] I. M. Dremin and J. W. Gary. *Phys. Lett.*, B459:341, 1999.
- [145] A. Capella et al. *Phys. Rev.*, D61:074009, 2000.
- [146] M. Boutemour. *Fortschr. Phys.*, 50:1001, 2002.